European Journal of Medicinal Chemistry 214 (2021) 113230

Contents lists available at ScienceDirect

European Journal of Medicinal Chemistry

journal homepage: http://www.elsevier.com/locate/ejmech

Design, synthesis and biological evaluation of pyrazole-aromatic containing carboxamides as potent SDH inhibitors

Bin Yu [a], Bin Zhao [c], Zesheng Hao [a], Lei Chen [a], Lixin Cao [a], Xiaofeng Guo [b, *], Nailou Zhang [a], Dongyan Yang [a, **], Liangfu Tang [a], Zhijin Fan [a, ***]

[a] State Key Laboratory of Elemento-Organic Chemistry, College of Chemistry, Nankai University, Tianjin, 300071, PR China
[b] College of Biology, Hunan University, Changsha, 410082, PR China
[c] College of Plant Protection, Hebei Agricultural University, Baoding, 071001, PR China

ARTICLE INFO

Article history:
Received 28 March 2020
Received in revised form
4 January 2021
Accepted 23 January 2021
Available online 1 February 2021

Keywords:
Succinate dehydrogenase inhibitors
Antifungal activity
Structure-activity relationships
Molecular docking

ABSTRACT

To continue our ongoing studies on discovery of new potent antifungal leads, 43 novel pyrazole-aromatic containing carboxamides were rationally designed and synthesized. Bioassays indicated that most target compounds displayed good *in vitro* antifungal activities against *Botrytis cinerea, Rhizoctonia cerealis* and *Sclerotinia sclerotiorum* and *in vivo* antifungal activity against *R. solani*. Compound **11ea** exhibited the most significant *in vitro* activity against *R. cerealis* (EC_{50} = 0.93 μg/mL) with about 2-fold more potent than a previously reported lead compound **A1** (EC_{50} = 2.01 μg/mL), and about 11-fold more potent than the positive control/commercial succinate dehydrogenase inhibitor thifluzamide (EC_{50} = 23.09 μg/mL). Structure-activity relationship analysis and molecular docking simulations indicated that the presence of difluoromethyl pyrazole-(*m*-benzene) carboxamide scaffold obviously increased the antifungal activity. The further enzymatic bioassay showed that both thifluzamide and compound **11ea** displayed excellent SDH inhibitory effects, and fluorescence quenching analysis suggested that they may share the same target SDH.

1. Introduction

Plant diseases caused by phytopathogens pose a worldwide threat to crop production and food security, fungicides played an effective role in crop diseases control and plant protection [1]. Among the over 50 classes of fungicides categorized by the Fungicide Resistance Action Committee (FRAC), succinate dehydrogenase inhibitor (SDHI) has been the fastest growing class of fungicides, which have been discovered and launched into the agrochemical market for the past decades [2,3]. The primary mode of action of SDHIs is to block the tricarboxylic acid cycle (TCA cycle) between succinate and fumarate thereby inhibiting the respiration of fungi, and leading to fungi death [2,3]. Due to its unique mode of action and broad-spectrum antifungal activity, SDHIs have attracted a wide range of research in discovering novel antifungal products [4–9], and potent anticancer agents [10]. However, SDHIs have been unrestrictedly used for plant protection since the first commercial product carboxin launched in 1966 [11], directly resulting in the development of fungi resistance [2,12,13]. Therefore, it is always necessary for modern plant protection to develop novel SDHI with different scaffolds to prevent cross-resistance.

Pyrazole derivatives, as an important class of nitrogen-containing heterocyclic compounds, have exhibited a wide variety of activities, including anti-inflammatory [14], anticancer [15], antifungal activities [16], etc. [17,18]. The representative SDHI fungicides including fluxapyroxad, benzovindiflupyr, bixafen, penflufen, sedaxane, penthiopyrad and isopyrazam share a pyrazole substructure (Fig. 1).

In our previous work, a series of novel pyrazole-thiazole containing carboxamides were synthesized and discovered with antifungal activity, especially against *Rhizoctonia cerealis* [19]. To continue our ongoing work on the discovery of novel fungicide, new pyrazole-thiazole carboxamides with various amine moieties were widely investigated, and a previous representative

* Corresponding author. State Key Laboratory of Elemento-Organic Chemistry, College of Chemistry, Nankai University, No. 94, Weijin Road, Nankai District, Tianjin, 300071, PR China.
** Corresponding author.
*** Corresponding author.
E-mail addresses: guoxf@hnu.edu.cn (X. Guo), yangdy@nankai.edu.cn (D. Yang), fanzj@nankai.edu.cn (Z. Fan).

https://doi.org/10.1016/j.ejmech.2021.113230
0223-5234/

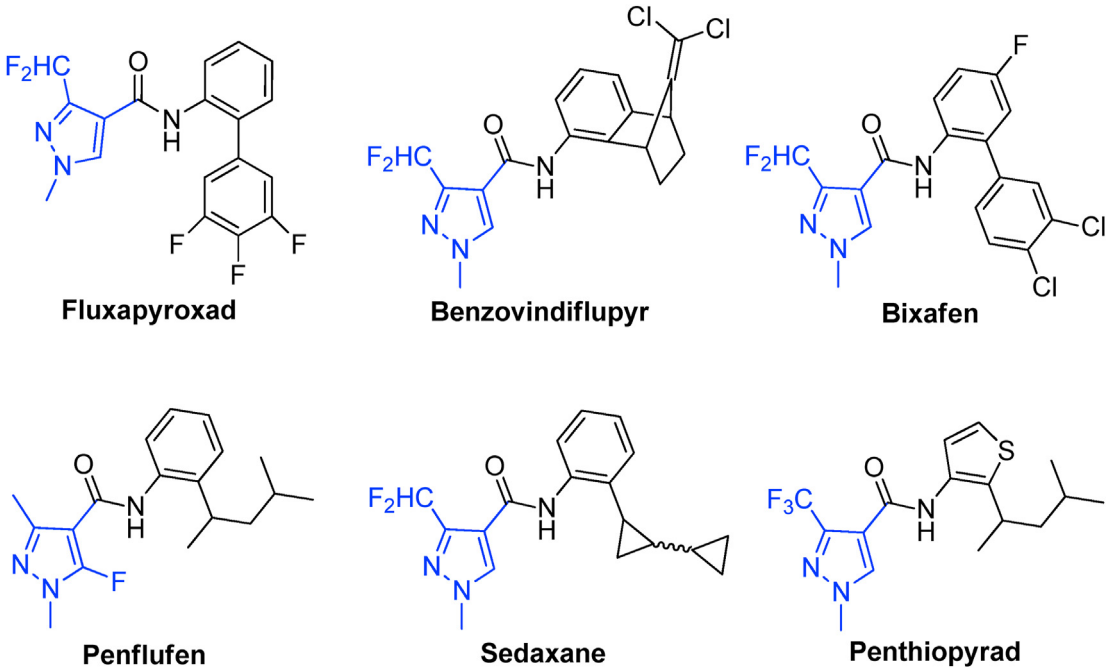

Fig. 1. Structures of the representative pyrazole containing SDH inhibitors.

lead compound **A1** was docked into the *R. cerealis* SDH active pocket. It was found that difluoromethyl-pyrazole group played an important role in the binding mode, because the $-CHF_2$ group formed an additional hydrogen bond with C-Arg81, and the pyrazole-thiazole moiety formed π-π interactions with B-His246 and B-Trp203, respectively (Fig. 2). On this basis, we supposed that the π-π interactions between the key residues and inhibitors might be a main contribution to increase antifungal activity. To prove our hypothesis, the pyrazole group was retained and the thiazole ring conjugated with pyrazole was replaced to improve the π-π interactions with the key residues in the binding site, thus, novel pyrazole-aromatic containing carboxamides (Fig. 3) were designed and synthesized. Experimental results discovered a new more potent compound **11ea** with better antifungal activity against *R. cerealis* than the positive control thifluzamide.

2. Results and discussion

2.1. Chemistry

The synthetic procedures of the key intermediates **10a-10e** are illustrated in Schemes 1-**3**. The commercially available compound **1** was used as a starting material to react with oxalyl chloride for affording the corresponding acyl chloride. Amide **2** was obtained by reaction of this acyl chloride with aqueous ammonia solution. The oxygen atom of compound **2** was substituted by S atom via Lawesson's reagent to obtain the thioamide **3**. Subsequently, the thioamide **3** and amide **2** were reacted with ethyl bromopyruvate by an intermolecular cyclization to give intermediate thiazole **9a** and oxazole **9b**, respectively (Scheme 1).

Carboxylic acid **1** was treated with diphenyl phosphorazidate (DPPA) in the presence of *t*-BuOH by a Curtius rearrangement to form the intermediate **4** [20] for further deprotection under an acidic condition to yield the amine **5**, followed by a Sandmeyer reaction, the intermediate **6** was obtained. Afterwards, the compound **7** was synthesized by reacting compound **6** with isopropoxyboronic acid pinacol ester in the presence of n-C_4H_9Li. Boronic esters **7** was subjected to the Suzuki coupling in the presence of $Pd(PPh_3)_4$ to form the intermediate **9c** (Scheme 1).

Commercially available compounds **8** and corresponding phenylboronic acids were subjected to Suzuki coupling in the presence of $PdCl_2$(dppf) to form the intermediates **9d** and **9e**, respectively.

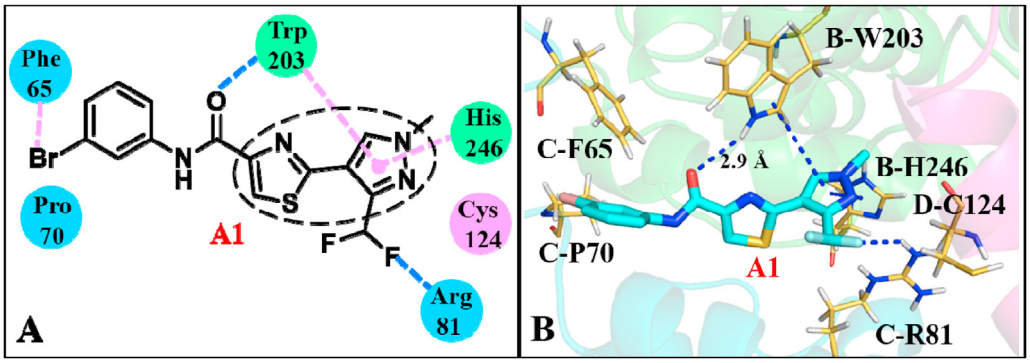

Fig. 2. Predicted binding mode of compound **A1** (A and B) with *R. cerealis* SDH.

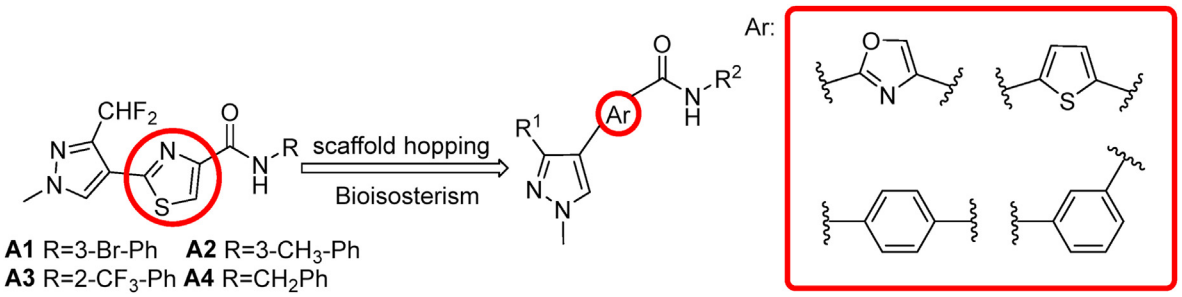

Fig. 3. Design strategy of the target compounds.

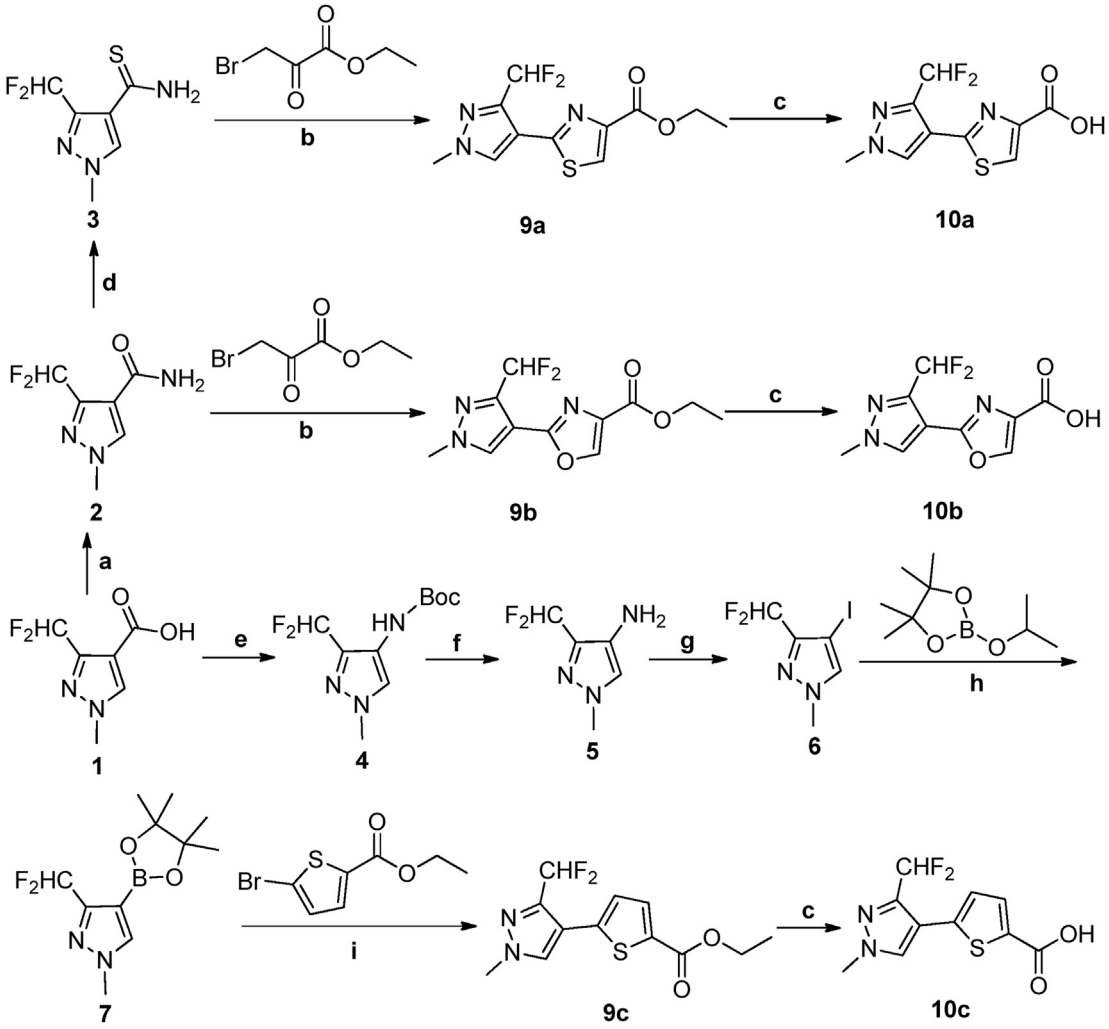

Scheme 1. Synthesis of the intermediates **10a-10b**. Reagents and conditions: **a**. $(COCl)_2$/DMF/CH_2Cl_2, $NH_3 \cdot H_2O$/CH_2Cl_2; **b**. EtOH, reflux; **c**. NaOH, EtOH/H_2O; **d**. Lawesson's reagent, THF, reflux, 1 h; **e**. DPPA, DIPEA, *t*-BuOH; **f**. TFA, CH_2Cl_2; **g**. 4 M HCl, $NaNO_2$, KI; **h**. *n*-C_4H_9Li, THF, −78 °C; **i**. 2 N Na_2CO_3, $Pd(PPh_3)_4$, reflux.

Finally, intermediates **9a-9e** were saponified with a 2 mol/L NaOH solution and subsequently acidified with a 2 mol/L HCl solution to give the carboxylic acids **10a-10e** (Scheme 2).

The target compounds **11aa-11eh** were synthesized according to the reaction route described in Scheme 3. The key intermediates **10a-10e** were combined with corresponding amine to yield the title compounds **11aa-11eh**. The structures of all of the target compounds were characterized by proton nuclear magnetic resonance (^{1}H NMR), carbon-13 nuclear magnetic resonance (^{13}C NMR) spectroscopies and high-resolution mass spectrometry (HRMS).

The crystal structure of the compound **11ea** (CCDC: 1962907) was identified by single crystal X-ray diffraction analysis as shown in Fig. 4 and Table S1 for further structure validation.

2.2. Biological evaluation

2.2.1. In vitro antifungal activity

All target compounds were evaluated for their *in vitro* antifungal activities against the nine representative plant fungi at a concentration of 50 μg/mL according to our previously reported method

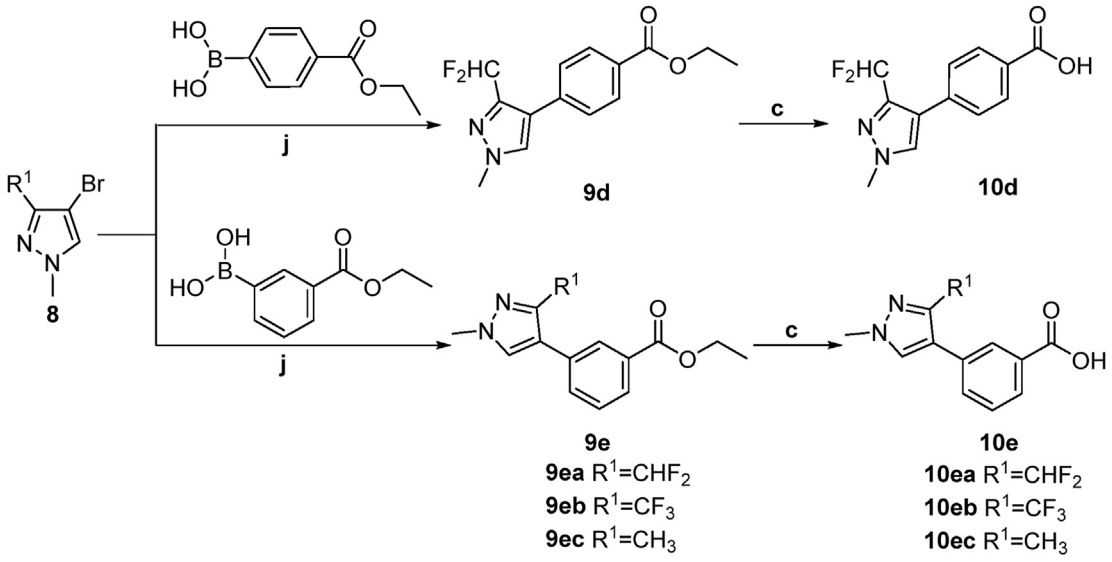

Scheme 2. Synthesis of the intermediates **10d-10e**. Reagents and conditions: **c**. NaOH, EtOH/H_2O; **j**. $PdCl_2$(dppf), Cs_2CO_3, reflux.

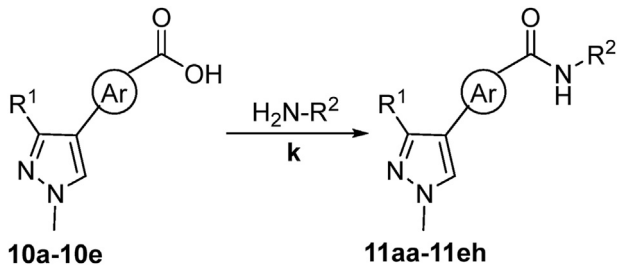

Scheme 3. Synthesis of the target compounds **11aa-11eh**. Reagents and conditions: **k**. PyBOP, DIPEA, CH_2Cl_2, r.t, overnight.

[21]. Commercial fungicides thifluzamide and fluxapyroxad were selected as the positive controls. The preliminary screening results are listed in Table 1, indicating that all compounds showed various degrees of inhibitory activities against the tested fungi.

Extensive investigation on the effects of various substituted anilines and amines on pyrazole-thiazole carboxamide scaffold (**11aa-11ay**) revealed that most compounds displayed moderate to good antifungal activities against *Botrytis cinerea*, *Cercospora arachidicola, Rhizoctonia cerealis*, and *Sclerotinia sclerotiorum*. For *B. cinerea*, compounds **11aa**, **11aj**, and **11aw** exhibited good activity with inhibitory effects more than 75%. Notably, the inhibition rate of compound **11aw** reached 83.8%, which was comparable to that of the positive control fluxapyroxad (87.3%). For *S. sclerotiorum*,

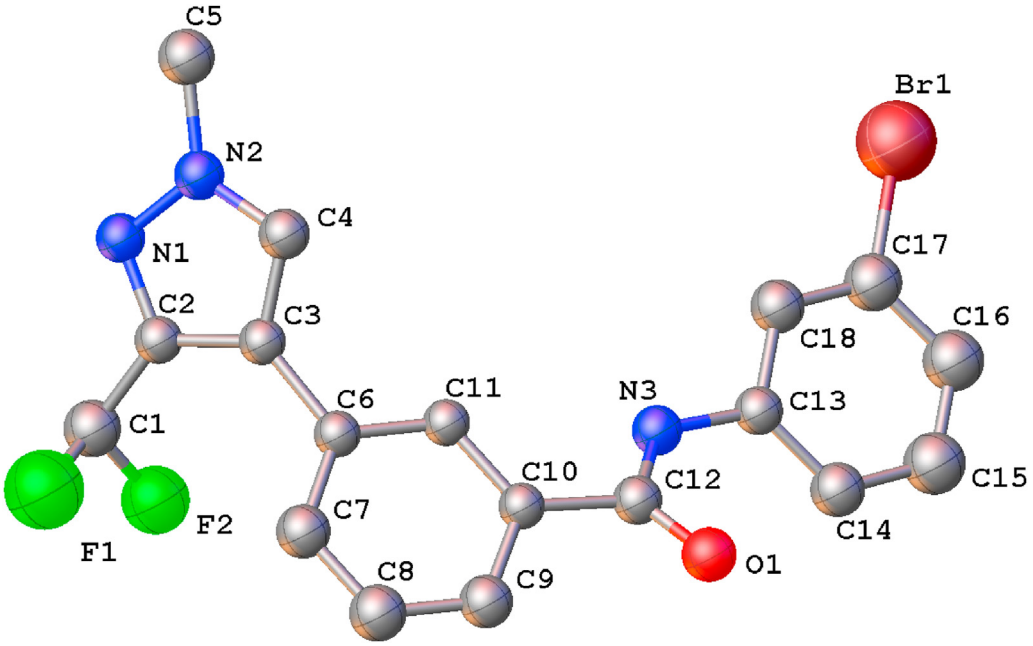

Fig. 4. Crystal structure of compound **11ea** (CCDC: 1962907).

Table 1
Chemical structures and *in vitro* antifungal activity of the target compounds **11aa-11eh** at 50 μg/mL.

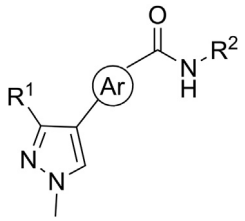

Compd	R^1	Ar	R^2	Inhibition rate[a] (%)								
				A.s[b]	*B. c*	*C. a*	*G. z*	*P. i*	*P. p*	*P. s*	*R. c*	*S. s*
11aa	CHF_2	thiazole	2-Cl-Ph	48.1	78.4	44.8	50.0	12.0	35.7	25.3	21.2	35.3
11 ab	CHF_2	thiazole	3-Cl-Ph	22.2	13.5	27.6	44.4	25.3	0	32.5	53.0	23.5
11ac	CHF_2	thiazole	4-Cl-Ph	66.7	45.9	51.7	88.9	38.7	21.7	54.2	54.5	35.3
11ad	CHF_2	thiazole	2-OMe-Ph	33.3	51.4	51.7	44.4	46.7	38.5	49.4	0	47.1
11ae	CHF_2	thiazole	3-OMe-Ph	14.8	18.9	10.3	22.2	17.3	21.7	18.1	15.2	17.6
11af	CHF_2	thiazole	4-OMe-Ph	3.7	62.2	17.2	33.3	49.3	14.7	13.3	15.2	23.5
11 ag	CHF_2	thiazole	2-OCF_3-Ph	70.4	73.0	75.9	66.7	57.3	56.6	42.2	60.6	52.9
11ah	CHF_2	thiazole	3-OCF_3-Ph	18.5	67.6	24.1	50.0	36.0	7.7	18.1	45.5	52.9
11ai	CHF_2	thiazole	4-OCF_3-Ph	25.9	29.7	10.3	50.0	12.0	7.7	0	0	0
11aj	CHF_2	thiazole	2-*i*Pr-Ph	39.1	77.8	59.0	39.2	44.3	53.6	51.5	88.9	83.3
11ak	CHF_2	thiazole	3,5-Br_2-Ph	14.3	34.5	15.5	42.9	0	13.4	28.1	41.8	71.4
11 al	CHF_2	thiazole	3,4-Cl_2-Ph	18.5	45.9	13.8	27.8	12.0	13.3	22.9	10.6	5.9
11am	CHF_2	thiazole	3,5-Cl_2-Ph	74.1	67.6	69.0	66.7	17.3	63.6	25.3	57.6	47.1
11an	CHF_2	thiazole	cyclopropane	0	45.9	3.4	22.2	14.7	18.9	0	12.1	17.6
11ao	CHF_2	thiazole	cyclohexane	55.6	13.5	62.1	61.1	30.7	46.9	44.6	63.6	17.6
11ap	CHF_2	thiazole	1-naphthalen	37.0	56.8	72.4	27.8	49.3	0.7	42.2	45.5	29.4
11aq	CHF_2	thiazole	1-(1,2,3,4-tetrahydronaphthalene)	22.2	0	17.2	27.8	25.3	21.7	32.5	50.0	0
11ar	CHF_2	thiazole	2-(5,6,7,8-tetrahydronaphthalene)	40.7	67.6	34.5	44.4	30.7	13.3	13.3	0	41.2
11as	CHF_2	thiazole	2-pyridine	77.8	67.6	72.4	66.7	57.3	60.8	30.1	53.0	64.7
11 at	CHF_2	thiazole	4-pyridine	3.7	73.0	10.3	27.8	9.3	18.9	37.3	12.1	94.1
11au	CHF_2	thiazole	3-Br-4-pyridine	11.1	73.0	13.8	38.9	14.7	59.4	8.4	15.2	64.7
11av	CHF_2	thiazole	4-pyrimidine	3.7	67.6	20.7	22.2	20.0	28.7	25.3	15.2	17.6
11aw	CHF_2	thiazole	2-pyrazine	59.3	83.8	58.6	55.6	52.0	27.3	25.3	33.3	41.2
11ax	CHF_2	thiazole	2-thiazole	3.7	73.0	24.1	11.1	12.0	13.3	3.6	22.7	17.6
11ay	CHF_2	thiazole	4-Me-2-thiazole	29.6	67.6	0	11.1	25.3	7.7	13.3	45.5	5.9
11ba	CHF_2	oxazole	3-Br-Ph	43.5	58.7	38.5	27.5	29.9	38.1	21.2	73.3	73.6
11bb	CHF_2	oxazole	3-Me-Ph	30.4	65.1	28.2	31.4	13.4	29.8	21.2	64.4	62.5
11bc	CHF_2	oxazole	2-CF_3-Ph	15.2	34.9	10.3	15.7	0	32.1	9.1	31.1	62.5
11ca	CHF_2	thiophene	3-Br-Ph	47.8	66.7	59.0	37.3	38.1	28.6	36.4	82.2	83.3
11 cb	CHF_2	thiophene	3-Me-Ph	52.2	65.1	48.7	37.3	36.1	45.2	39.4	90.0	80.6
11da	CHF_2	*p*-benzene	3-Br-Ph	56.5	74.6	28.2	56.9	36.1	40.5	45.5	82.2	93.1
11 db	CHF_2	*p*-benzene	3-Me-Ph	41.3	71.4	38.5	41.2	19.6	16.7	27.3	84.4	76.4
11dc	CHF_2	*p*-benzene	2-CF_3-Ph	10.9	34.9	7.7	33.3	7.2	2.4	15.2	22.2	66.7
11dd	CHF_2	*p*-benzene	$PhCH_2$	8.7	33.3	5.1	13.7	1.0	2.4	9.1	31.1	72.2
11de	CHF_2	*p*-benzene	3-CF_3-Ph	13.0	28.6	17.9	5.9	1.0	7.1	15.2	16.7	72.2
11ea	CHF_2	*m*-benzene	3-Br-Ph	71.7	74.6	66.7	56.9	46.4	27.4	42.4	94.4	95.8
11eb	CHF_2	*m*-benzene	3-Me-Ph	39.1	49.2	33.3	35.3	9.3	14.3	3.0	51.1	91.7
11ec	CHF_2	*m*-benzene	2-CF_3-Ph	30.4	57.1	28.2	45.1	9.3	14.3	15.2	42.2	70.8
11ed	CHF_2	*m*-benzene	$PhCH_2$	30.4	58.7	28.2	17.6	19.6	9.5	39.4	64.4	66.7
11ee	CF_3	*m*-benzene	3-Br-Ph	28.6	36.1	15.5	17.9	0	4.9	15.6	28.6	50.0
11ef	CF_3	*m*-benzene	3-Me-Ph	23.8	29.4	15.5	25.0	0	9.8	21.9	28.6	67.9
11eg	CF_3	*m*-benzene	2-*i*Pr-Ph	85.7	45.4	83.1	0	39.3	23.2	53.1	94.9	85.7
11eh	CH_3	*m*-benzene	3-Me-Ph	63.0	74.5	65.7	56.8	40.4	67.9	32.7	90.8	76.9
Fluxapyroxad				73.9	87.3	100	41.2	13.4	47.6	15.2	41.1	83.3
Thifluzamide				65.2	58.7	82.1	35.3	13.4	39.3	15.2	55.6	87.5

[a] Values are the mean of three replicates.
[b] Abbreviations: *A. s*: *Alternaria solani*; *B. c*: *Botrytis cinerea*; *C. a*: *Cercospora arachidicola*; *G. z*: *Gibberella zeae; P. i*: *Phytophthora infestans* (Mont) de Bary; *P. p*: *Physalospora piricola*; *P. s*: *Pellicularia sasakii*; *R. c*: *Rhizoctonia cerealis*; and *S. s*: *Sclerotinia sclerotiorum.*

compounds **11aj**, **11ak**, and **11 at** showed more than 70% inhibitory activity. Particularly, the compound **11 at** showed the highest inhibition effect (94.1%), which was superior to that of the positive controls thifluzamide (87.5%) and fluxapyroxad (83.3%). Moreover, compound **11aj** displayed remarkably higher antifungal activity (88.9%) than that of thifluzamide (55.6%) against *R. cerealis*. For *C. arachidicola*, although compound **11 ag** exhibited the highest antifungal activity (75.9%), it was still lower than those of thifluzamide (82.1%) and fluxapyroxad (100%).

Meanwhile, to further explore an optimal aromatic ring to replace the middle thiazole ring, *in vitro* antifungal activities of the synthesized compounds **11ba-11eh** were also evaluated, and the

results were illustrated in Table 1. It was worth noting that these novel compounds showed good to excellent inhibitory effects against *B. cinerea*, *R. cerealis* and *S. sclerotiorum*. Based on the results of preliminary screening, all compounds **11ba-11eh** and several compounds from **11aa-11ay** were chosen for their median effective concentration (EC_{50}) determination and comparison with the lead compound **A1**. The results shown in Table 2 revealed that, these compounds showed different inhibitory activities against the three tested fungi. For *R. cerealis*, most compounds including **11aj**, **11ba**, **11ca**, **11da**, **11ea**, **11eb**, and **11eg** showed significantly stronger inhibitory activity with EC_{50} values ranging from 0.93 to 4.50 μg/mL. They were more potent than thifluzamide with an EC_{50} value of 23.09 μg/mL. Among them, **11ea** was the most active one with the lowest EC_{50} value of 0.93 μg/mL. It was superior to thifluzamide and about 2-fold more active than the lead compound **A1** with an EC_{50} value of 2.01 μg/mL. For *B. cinerea*, **11ba**, **11ca**, **11 cb**, **11 db**, and **11ea** exhibited stronger inhibitory activity with EC_{50} values ranging from 2.03 to 9.78 μg/mL. They were more potent than thifluzamide with an EC_{50} value of 11.65 μg/mL. Among these, **11 cb** showed the most potent activity with an EC_{50} value of 2.03 μg/mL. It was about 6-fold more active than thifluzamide. For *S. sclerotiorum,* **11da**, **11ea**, **11ee**, and **11eg** exhibited notably higher antifungal activity with EC_{50} values ranging from 0.51 to 1.64 μg/mL. They were more potent than thifluzamide with an EC_{50} value of 4.88 μg/mL. In particular, **11eg** showed the strongest activity with the lowest EC_{50} value of 0.51 μg/mL. It was about 9-fold more active than thifluzamide.

2.2.2. SAR according to in vitro antifungal activity

Based on the results in Tables 1 and 2, SAR of novel derivatives was analyzed. By comparing the inhibition rates of **11aa-11am** in Table 1, the antifungal activities were varied with regard to the different groups and different substituents on the phenyl ring. The compounds with a *meta*- or an *ortho*-substituent on the phenyl ring exhibited better activity against most tested fungi than compounds with a *para*-substituent. For example, trifluoromethoxy group in **11 ag** and **11 ah** at the *ortho*- or *meta*-position of the phenyl ring were favorable for the inhibitory activity against all tested fungi. Compound **11ad** with a methoxy group at the *ortho*-position of the phenyl group also showed better inhibitory activity against the most tested fungi as compared with the compound **11af** bearing such a group on *para*-position. Moreover, an introduction of 3,5-Cl_2 groups in **11am** showed significant activity improvement against almost all tested fungi as compared with the monosubstituted compound **11 ab**. In contrast, the presence of 3,4-Cl_2 in **11 al** obviously decreased the inhibitory activity. These results indicated that there may exist a steric hindrance between the *para*-substituent of the benzene ring and SDH, which affected the bioactive conformation of the inhibitor, thereby significantly reduced its potency. Interestingly, an opposite trend was observed among **11aa-11ac**. Compound **11ac** containing *para*-substituted chlorine displayed stronger inhibitory activity than **11aa** and **11 ab** against almost all tested fungi. These results suggested that the steric effect of chlorine appeared not to be the main factor affecting its antifungal activity of monochlorinated compounds. In addition, the structures of amines (**11an**-**11ay**) also played an important role on the antifungal activity. It was concluded that compounds containing a six-membered aromatic ring generally exhibited higher activity than compounds containing other rings such as an aliphatic ring in **11an**, a tetrahydronaphthalene ring in **11aq**, **11ar**, or a five-membered aromatic ring in **11ax**, **11ay**. Among the six-membered aromatic compounds, **11as** (R^2 = 2-pyridine) showed a broad spectrum of antifungal activity (exhibited >50% activity against eight fungi). Compound **11 at** (R^2 = 4-pyridine) exhibited excellent activity against *S. sclerotiorum* (94.1%). In comparison with **11 at**, an introduction of 3-Br in **11au** on the 4-pyridine group slightly increased inhibitory activity against most of the tested fungi, but reduced the inhibitory activity against *S. sclerotiorum*.

The *in vitro* antifungal activity of **11ba-11eh** are listed in Tables 1 and 2, most of the compounds exhibited good to excellent inhibitory activity against *B. cinerea*, *R. cerealis* and *S. sclerotiorum*. The results of selected compounds in **11aa-11ay** are listed in Table 2. **11ak** (R^2 = 3,5-Br_2-Ph) showed a remarkably decrease in antifungal activity against *R. cerealis* as compared with the compound **A1**, indicating that the mono substituted group at *ortho*- or *meta*-position on the phenyl ring might be more favorable for the inhibitory activity than the disubstituted group. Notably, **11aj** exhibited similar activity against *R. cerealis* as compared with **A1**, suggesting that introducing a bulky hydrophobic group at *ortho*- or *meta*-position on the phenyl ring may also afford potent inhibitors, its molecular mechanism would be discussed in the following section. For **11ba-11eh**, the EC_{50} values revealed that certain compounds such as **11 cb** (Ar = thiophene), **11 db** (Ar = *p*-benzene) and **11ea**, **11eb**, **11ed** (Ar = *m*-benzene) showed promising activity against *R. cerealis* as compared with the corresponding pyrazole-thiazole compounds **A1**, **A2**, **A3**, or **A4**. Among them, **11ea** showed the best potency against *R. cerealis*, which was superior to the positive control thifluzamide and the lead compound **A1**, indicating that the benzene ring might increase the π-π interaction with key residues in *Rc*SDH active site. Surprisingly, **11ea** also exhibited remarkably antifungal activities against *B. cinerea* and *S. sclerotiorum* with EC_{50} values of 3.85 and 0.85 μg/mL, respectively. These were superior to thifluzamide. Moreover, **11ba** (Ar = oxazole) and **11da** (Ar = *p*-benzene) showed stronger inhibitory activity against *R. cerealis* than thifluzamide. By conclusion, SAR of **11ba-11eh** against *R. cerealis* displayed a trend: *m*-benzene > *p*-benzene > thiophene > oxazole, these results confirmed the importance of the π-π interaction between the pyrazole-aromatic moiety of the ligand and the key residues of SDH, as hypothesized in our molecular design.

After *in vitro* antifungal activity confirmed that the scaffold of pyrazole-(*m*-benzene) carboxamide could be selected as a lead structure for further modification, we further modified the 3-position of the pyrazole ring by replacing R^1 = $-CHF_2$ with R^1 = $-CF_3$ or $-CH_3$. Disappointedly, the inhibitory activity of **11ee-11eh** against *R. cerealis* significantly decreased, suggesting that the difluoromethyl group at R^1 would be more favorable for the antifungal activity. Surprisingly, the inhibitory activity of **11eg** against *S. sclerotiorum* increased considerably.

To understand the structure-activity relationship of these novel pyrazole-aromatic containing carboxamides at atomic level, the positive control thifluzamide and selected compounds (**11ea**, **11ai**, **11aj**, and **11ak**) were docked into the theoretical active site of modeled *Rc*SDH, respectively. As described in Fig. 5A, thifluzamide was bound in the active pocket of *Rc*SDH, the key residue B-Trp203 formed a hydrogen bond with the carbonyl oxygen atom, which was crucial for the binding between the inhibitor and *Rc*SDH. The nitrogen atom of thiazole moiety formed an additional hydrogen bond with C-Arg81. Meanwhile, the thiazole ring formed a weak π-π stacking interaction with B-His246. The aniline moiety was stretched into the hydrophobic pocket that consisted of the residues C-Phe65, C-Trp74, and C-Ile78. However, the trifluoromethoxy group at the 4-position of the benzene ring existed steric repulsion with the residues in the hydrophobic pocket. Moreover, the presence of a methyl substituent at the 2-position of the thiazole ring led to unfavorable repulsion with D-Asp127, which may account for its relative weaker antifungal potency.

The simulated binding mode of potent compound **11ea** (Fig. 5B) showed that the carbonyl oxygen atom also formed a hydrogen bond with the key residue B-Trp203 and pyrazole ring formed a stacking π-π interaction with the residue B-His246, which were similar to the thifluzamide. In addition, a fluorine atom of the

Table 2
Chemical structures and antifungal potency of the target compounds **11aa-11eh** against *B. cinerea*, *R. cerealis* and *S. sclerotiorum*.

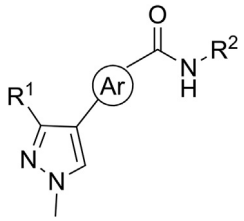

Compd.	R^1	Ar	R^2	EC_{50}[a] (μg/mL)		
				B. cinerea	*R. cerealis*	*S. sclerotiorum*
A1 [19]	CHF_2	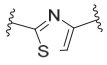	3-Br-Ph	-	2.01	-
A2 [19]	CHF_2	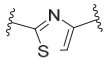	3-CH_3-Ph	-	6.23	-
A3 [19]	CHF_2	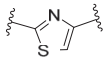	2- CF_3-Ph	-	10.04	-
A4 [19]	CHF_2	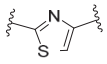	CH_2Ph	-	20.07	-
11aj	CHF_2	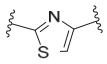	2-*i*Pr-Ph	24.94	2.77	47.13
11ak	CHF_2	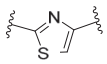	3,5-Br_2-Ph	>100	30.99	25.24
11 at	CHF_2	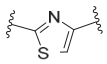	4-pyridine	-	-	7.01
11aw	CHF_2	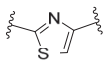	2-pyrazine	46.1	-	-
11ba	CHF_2	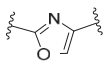	3-Br-Ph	9.78	2.67	35.64
11bb	CHF_2	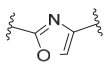	3-Me-Ph	34.58	14.13	42.94

(*continued on next page*)

Table 2 (*continued*)

Compd.	R^1	Ar	R^2	EC_{50}[a] (μg/mL)		
				B. cinerea	*R. cerealis*	*S. sclerotiorum*
11bc	CHF_2	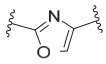	2-CF_3-Ph	>100	>100	19.97
11ca	CHF_2	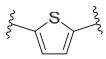	3-Br-Ph	4.18	4.50	16.67
11 cb	CHF_2	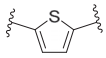	3-Me-Ph	2.03	6.41	17.39
11da	CHF_2	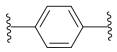	3-Br-Ph	12.73	2.19	1.32
11 db	CHF_2	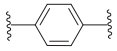	3-Me-Ph	4.86	7.09	5.19
11dc	CHF_2	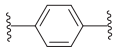	2-CF_3-Ph	>100	>100	65.38
11dd	CHF_2	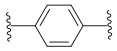	$PhCH_2$	14.00	>100	12.83
11de	CHF_2	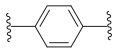	3-CF_3-Ph	17.96	8.60	5.16
11ea	CHF_2	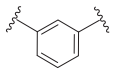	3-Br-Ph	3.85	0.93	0.85
11eb	CHF_2	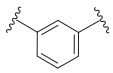	3-Me-Ph	>100	4.20	14.88
11ec	CHF_2	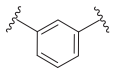	2-CF_3-Ph	38.28	19.19	15.84
11ed	CHF_2	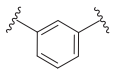	$PhCH_2$	43.09	19.28	45.81
11ee	CF_3	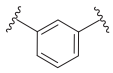	3-Br-Ph	>100	>100	1.64
11ef	CF_3	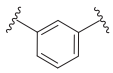	3-Me-Ph	>100	>100	12.62
11eg	CF_3	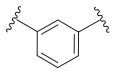	2-*i*Pr-Ph	-	3.17	0.51
11eh	CH_3	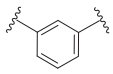	3-Me-Ph	33.17	9.94	16.15
Thifluzamide				11.65	23.09	4.88

[a] Values are the mean of three replicates. "-" = No test.

difluoromethyl group formed another hydrogen bond with C-Arg81 and pyrazole ring formed a T-shaped π-π interaction with B-Trp203. The 3-Br substituted aniline moiety was stretched through the hydrophobic pocket that consists of C-Pro70 and C-Ile78, and its bromine atom formed a cation-π interaction with C-Phe65. The superimposition of **11ea** and **A1** (Fig. 5C) showed a similar pattern in the SDH active site. The middle benzene ring of **11ea** adjusted its binding mode, which in favor of the π-π interactions with both B-His246 and B-Trp203 and the hydrogen bond with B-Trp203. Altogether, the aforementioned interactions may contribute to the stabilization of **11ea** and analogs in *Rc*SDH active site.

The presence of trifluoromethoxy group on the benzene ring (**11ai**) resulted in poor activity due to steric hindrance with C-Tyr68, C-Gln69 and C-Pro70 (Fig. 5D). Besides, **11ai** failed to form the crucial hydrogen bond with B-Trp203. Notably, compared with **11ea**, the high potency of compound **11aj** (Fig. 5E) was attributed to an additional hydrogen bond (C-F···H interaction) with C-Arg81, although the hydrogen bond (C=O···H interaction) of its carbonyl

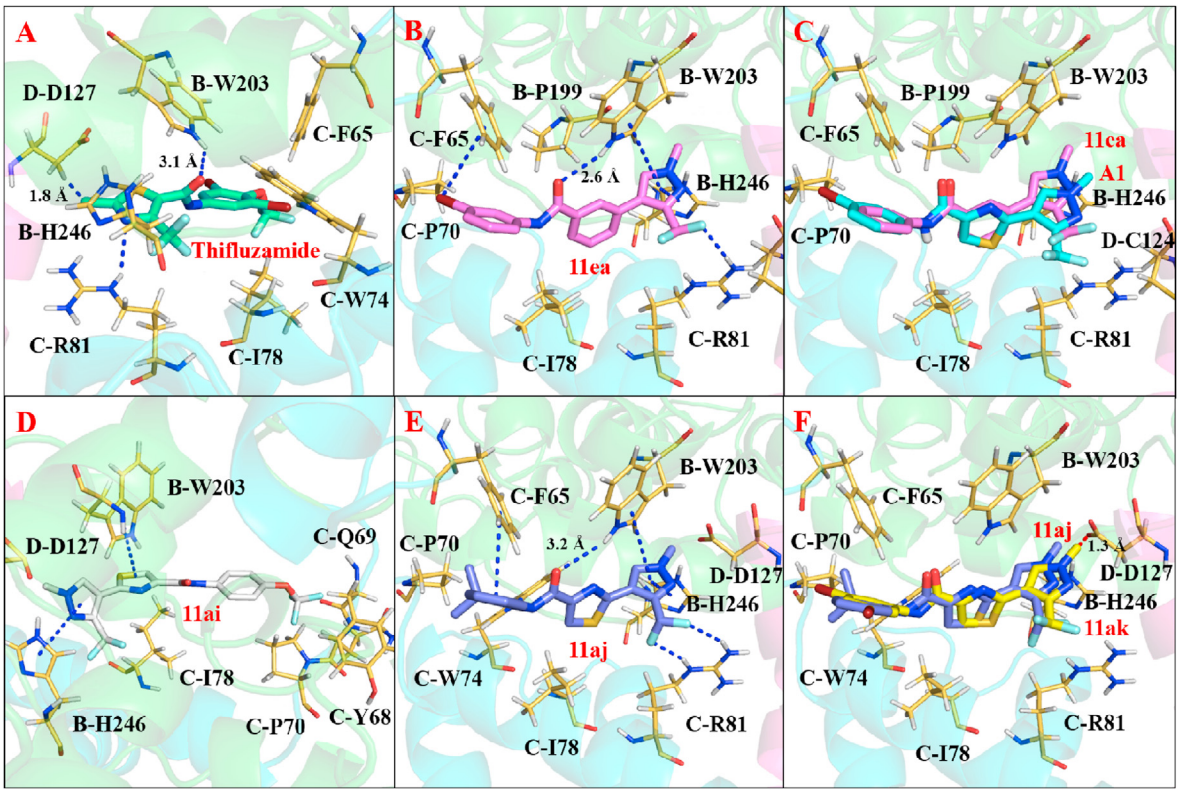

Fig. 5. Simulated binding mode of (A) **Thifluzamide** (lime green sticks) with *Rc*SDH, (B) compound **11ea** (magenta sticks) with *Rc*SDH; (C) the binding mode overlay of compound **11ea** and **A1** bonding with *Rc*SDH (represented by magenta and cyan sticks); the binding mode of (D) compound **11ai** (white sticks) with *Rc*SDH, (E) compound **11aj** (slate sticks) with *Rc*SDH; simulated binding mode overlay of compound **11aj** and **11ak** with *Rc*SDH (represented by slate and yellow sticks).

oxygen atom was weaker than that of **11ea**. Furthermore, the presence of isopropyl group on the benzene ring of **11aj** could improve the hydrophobic interaction. As shown by superimposition of **11aj** and **11ak** (Fig. 5F), the decreased activity of **11ak** was due to the steric repulsion with D-D127.

2.2.3. *In vivo* antifungal activity

The *in vivo* protective activities of **11aa-11eh** against *E. graminis*, *P. sorghi* Schw, *P. oryzae* and *R. solani* were further evaluated. Thifluzamide was chosen as a positive control. The results are listed in Table 3. Although most compounds showed lower antifungal activities (at 200 μg/mL) against *E. graminis*, *P. sorghi* Schw and *P. oryzae* than thifluzamide, some compounds still displayed good inhibitions against *P. sorghi* Schw (**11ba**, 75%; **11bb**, 98%; **11 db**, 75%) and *P. oryzae* (**11af**, 70%; **11ax**, 70%; **11ay**, 70%). Moreover, most compounds also displayed good to excellent activities against *R. solani* (**11aa-11 ay** at 200 μg/mL, **11ba-11eh** at 100 μg/mL). Among those, **11ca**, **11 cb**, **11 db**, **11eb**, and **11eg** exhibited over 80% inhibitory activity at 100 μg/mL, **11ca** exhibited slightly lower activity (70% inhibition at 10 μg/mL) than thifluzamide (80% inhibition at 10 μg/mL). Unfortunately, the potent compound **11ea** with good *in vitro* antifungal activity did not show the desired *in vivo* potency. UV irradiation and/or metabolism may be impacting factors for *in vivo* activity, which was worth for further study. These results indicated that these compounds exhibited promising activities against *R. solani in vivo*, and could be regarded as the new structural scaffolds for further optimization.

2.2.4. SDH enzyme activity as influenced by target compounds

R. cerealis SDH activity as influenced by compound **11ea** and several representative compounds were tested. The results listed in Table 4 showed that most selected compounds showed a decrease (at 10 μg/mL) in enzyme activity as compared with the lead compound **A1** (14.13 U/mg). Among them, **11aj** (10.96 U/mg) exhibited better enzyme activity than **11ak** (2.05 U/mg), **11eb** ($R^1 = -CHF_2$) displayed higher enzyme activity than **11eh** ($R^1 = -CH_3$), the enzyme activity showed the trends of **11da** (Ar = *p*-benzene) > **11ba** (Ar = oxazole) ≈ **11ca** (Ar = thiophene), these trends were very similar to the results of their *in vitro* antifungal activity against *R. cerealis*. However, **11ea** (6.10 U/mg) did not show the desired potency, the lower concentration determination for IC_{50} calculation shown in Table 5 indicated that **11ea** exhibited SDH enzymatic inhibition activity with an IC_{50} value of 1.49 μg/mL, even though it was less active than the positive control thifluzamide with its IC_{50} value of 0.49 μg/mL, it was obvious that they might act at the same target SDH.

2.3. Fluorescence quenching of SDH

To find the target of active compound with unknown mode of action, gene identification combined with molecular biology by bioinformatics and comprehensive omics is a good method [22,23]. Fluorescence quenching experiments can reveal the interactions between a protein and a ligand and identify the target of the active small molecule. Fluorescence quenching analysis of *R. cerealis* SDH was conducted with the compound **11ea**, thifluzamide and tricyclazole, which were used to validate interactions between protein and compounds. As shown in Fig. 6A, the fluorescence intensity of *R. cerealis* SDH was the strongest at 0 μg/mL (a, black curve) of **11ea**, and the weakest at 5 μg/mL (e, red curve) of **11ea**, that was, the fluorescence intensity of *Rc*SDH was gradually quenched as the concentration of compound **11ea** increased, which was similar to

Table 3
The *in vivo* antifungal activity of the target compounds **11aa-11eh**.

Compd	Inhibition rate[a] (%)					
	[b] *E. graminis*	[b] *P. sorghi* Schw	[b] *P. oryzae*	[b] *R. solani*	[c] *R. solani*	[d] *R. solani*
11aa	0	0	0	70	10	0
11 ab	0	20	0	90	30	20
11ac	70	50	50	100	40	30
11ad	0	0	0	40	-	-
11ae	0	0	0	100	70	0
11af	0	0	70	100	40	30
11 ag	0	0	0	90	-	-
11ah	0	0	0	70	-	-
11ai	20	20	0	70	-	-
11aj	0	20	0	100	0	-
11ak		50	0		50	-
11 al	0	20	0	100	-	-
11am	0	0	0	70	-	-
11an	0	0	0	100	-	-
11ao	0	0	0	50	-	-
11ap	0	0	0	60	-	-
11aq	0	0	0	60	-	-
11ar	0	0	0	80	0	-
11as	0	0	50	100	10	-
11 at	0	0	50	100	10	-
11au	20	0	50	100	0	-
11av	0	50	0	100	0	-
11aw	0	0	0	60	0	-
11ax	0	0	70	100	0	-
11ay	0	0	70	100	0	-
11ba	-	75	-	-	50	-
11bb	-	98	-	-	30	-
11bc	-	20	-	-	0	-
11ca	-	40	-	-	100	70
11 cb	-	20	-	-	80	60
11da	-	45	-	-	70	0
11 db	-	75	-	-	100	60
11dc	-	0	-	-	50	-
11dd	-	0	-	-	60	-
11de	-	20	-	-	30	-
11ea	-	10	-	-	10	-
11eb	-	0	-	-	100	0
11ec	-	40	-	-	50	-
11ed	-	50	-	-	10	-
11ee	-	10	-	-	40	-
11ef	-	0	-	-	10	-
11eg	-	10	-	-	80	70
11eh	-	40	-	-	70	50
Thifluzamide	98	100	50	100	90	80

[a] Values are the mean of three replicates
[b,c,d] Test concentration was 200, 100 and 10 μg/mL, respectively; Abbreviations: *E. graminis*: wheat white powder; *P. sorghi*: corn rust; *P. oryzae*: rice blast; *R. solani*: rice sheath blight.
"-" = No test.

Table 4
R. cerealis SDH enzyme activity at 10 μg/mL.

Compd.	SDH activity (U/mg)
A1	14.13
11aj	10.96
11ak	2.05
11ba	6.89
11ca	6.52
11da	12.56
11ea	6.10
11eb	10.63
11ec	5.68
11ed	8.46
11eh	5.68
Thifluzamide	2.48

the pattern of the positive control thifluzamide (Fig. 6B). In another aspect, there was no significant fluorescence change when treated by a negative control tricyclazole, a melanin synthesis inhibitor

Table 5
Inhibitory effect of **11ea** against *R. cerealis* SDH.

Compd	IC_{50} (μg/mL)	Regression equation	R^2
11ea	1.49	$y = 4.6768x + 1.8735$	0.9949
Thifluzamide	0.49	$y = 5.4044x + 1.3047$	0.9809

[24,25] (Fig. 6C). Compound **11ea** showed a similar pattern of fluorescence quenching as compared with thifluzamide, suggesting that they have the same mode of action.

3. Conclusion

In order to further investigate the impact of various amine moieties on pyrazole-thiazole carboxamide scaffold and different pyrazole-aromatic scaffolds on antifungal activity, forty-three novel pyrazole-aromatic containing carboxamides were designed, synthesized and evaluated against different fungi. The results indicated

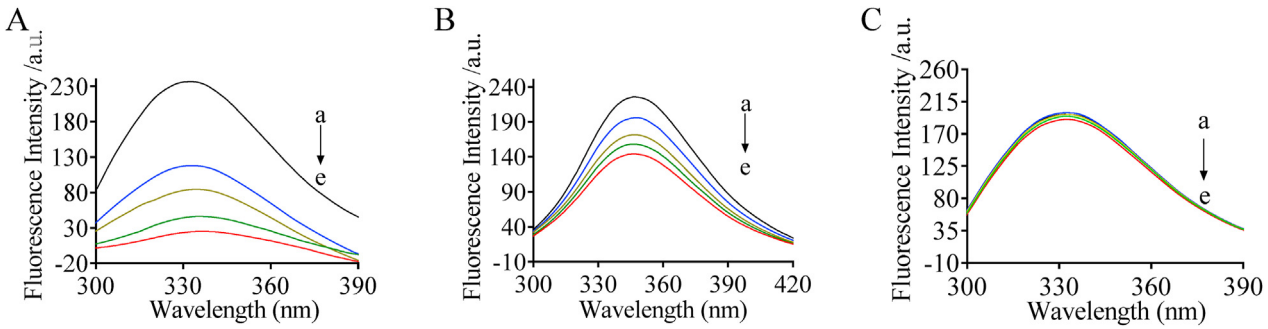

Fig. 6. Fluorescence spectra of SDH with **11ea**, thifluzamide or tricyclazole titration. (A) Fluorescence quenching analysis of compound **11ea** with SDH. (B) Fluorescence quenching analysis of **thifluzamide** with SDH. (C) Fluorescence quenching analysis of **tricyclazole** with SDH. The concentration of SDHI from "a to e" stands for "0–5 μg/mL.

that most of the target compounds displayed satisfactory *in vitro* antifungal activities, especially against *B. cinerea, R. cerealis*, *S. sclerotiorum* and *in vivo* antifungal activity against *R. solani*. The compounds with pyrazole-(*m*-benzene) carboxamide scaffold were more suited for improving activity against *R. cerealis*. And SAR analysis indicated that the promising antifungal potency of target compounds could be affected by structural changes, including an alteration of the amine moiety, replacement of the thiazole ring, and the modification of difluoromethyl substitution on the pyrazole ring. Among these compounds, compound **11ea** exhibited the most potent activity against *R. cerealis,* which was obviously better than both thifluzamide and the previous lead structure **A1**. The further enzymatic inhibitory activity and fluorescence quenching analysis of **11ea** suggested that SDH was the same target for both novel active compounds and thifluzamide. In addition, molecular docking simulations revealed that **11ea** binds with the active site of *Rc*SDH, formed a hydrogen bond with B-Trp203. Meanwhile, its difluoromethyl group formed an additional hydrogen bond with C-Arg81 and the pyrazole ring formed π-π interactions with both B-Trp203 and B-His246, thereby improving the potency of **11ea** against *Rc*SDH. According to the above analysis, we concluded that the difluoromethyl group at R^1 position would increase the binding affinity and the middle benzene ring could enhance the π-π interaction. Unfortunately, although there was no obvious phytotoxicity was observed, **11ea** showed lower *in vivo* activity against *R. solani* than thifluzamide, which may due to biological factors (e.g., plant metabolism, systemic) or/and environmental factors such as UV photolysis. Therefore, how to improve the *in vivo* antifungal activity and retain the active scaffold would be the primary concern in our future work. Overall, pyrazole-aromatic containing carboxamides were worthy for further structural optimization as potent SDHI fungicide leads.

4. Experimental section

4.1. Chemistry

All chemical reagents and solvents were commercially available and were used without further purification. Thin-layer chromatography (TLC) analysis was performed on silica gel F_{254} plates. Flash column chromatography was carried out on silica gel (200–300 mesh). ^{1}H NMR (400 MHz) and ^{13}C NMR (101 MHz) spectra were recorded on a Bruker Avance-400MHz spectrometer (Bruker, Switzerland) with TMS as an internal standard, deuterated chloroform ($CDCl_3$) or dimethyl sulfoxide (DMSO-d_6) as a solvent. The chemical shifts for the NMR spectra were reported in parts per million (ppm), the coupling constants (*J*) were described in hertz (Hz). Peak multiplicities were expressed as singlet (s), doublet (d), triplet (t), quartet (q), multiplet (m), double of doublet (dd) and double of triplet (dt). High resolution mass spectra (HRMS) were obtained from a Varion 7.0 T FTICR-MS instrument (Ion-Spec, USA). Melting points (m.p.) were determined on an X-4 digital display micro melting point apparatus (Henan Gongyi Yingyi Yuhua Instrument Co., Ltd.) and were uncorrected. Single-crystal X-ray diffraction analysis was performed on a Rigaku 007 Saturn 70 diffractionmeter (Rigaku, Tokyo, Japan). Fluorescence quenching analysis was conducted by a F-4500 fluorescence spectrophotometer (Hitachi, Tokyo, Japan).

4.1.1. Synthetic procedure for compound *2*

The synthesis procedure was adjusted according to the previously reported literature [19]. Oxalyl chloride (4.9 mL, 56.78 mmol) and 0.15 mL of *N*, *N*-dimethylformamide (DMF) were added to a suspension of compound **1** (5.0 g, 28.39 mmol) in dichloromethane (50 mL). The reaction mixture was stirred for 30 min at room temperature. After confirmation of the completion of the reaction, the solvent was removed, the crude residue was diluted with dry dichloromethane. Then the diluted solution was added dropwise to a 25% aqueous ammonia solution (7.72 g, 113.56 mmol) using a constant-pressure dropping funnel at 0 °C and the reaction suspension was stirred overnight at room temperature. After completion of the reaction, the suspension was filtration and evaporation to dryness. The crude product **2** (white solid, 4.6 g, 93%) was used directly in the next step without further purification.

4.1.2. Synthetic procedure for compound *3*

The synthesis procedure was adjusted according to the previously reported literature [19]. A suspension of intermediate **2** (9.00 g, 51.39 mmol) and Lawesson's reagent (12.73 g, 31.47 mmol) in 50 mL of tetrahydrofuran (THF) was heated to reflux at 65 °C for 30 min. After confirmation of the completion of the reaction by TLC, the solvent was removed under reduced pressure. The residue was diluted with ethyl acetate (30 mL) and sequentially washed with saturated K_2CO_3 (30 mL × 2) and brine (15 mL), and dried over anhydrous Na_2SO_4, then filtered and concentrated under reduced pressure. The crude product was purified by silica gel flash column chromatography with a solvent mixture of ethyl acetate and hexane (2:1, *v*/*v*) to afford thioamide **3** [19].

3-(Difluoromethyl)-1-methyl-1H-pyrazole-4-carbothioamide (**3**). Yellow solid; yield, 88%; m.p.: 135–137 °C.^{1}H NMR (400 MHz, $CDCl_3$) δ 8.23 (s, 1H), 7.76 (s, 1H), 7.58 (s, 1H), 6.79 (t, J = 54.1 Hz, 1H), 3.91 (s, 3H). ^{13}C NMR (101 MHz, $CDCl_3$) δ 191.4, 139.6 (t, J = 29.9 Hz), 139.4, 121.7, 112.1 (t, J = 232.7 Hz), 39.5. HRMS (ESI) *m*/*z* calcd for $C_6H_8F_2N_3S$ $[M + H]^+$: 192.0402; found: 192.0404.

4.1.3. Synthetic procedure for compound *9a*

The synthesis procedure was adjusted according to the previously reported literature [19]. The ethyl bromopyruvate (4.9 mL,

28.8 mmol) was added dropwise to a solution of intermediate **3** (5.0 g, 26.2 mmol) in ethanol at room temperature. The reaction mixture was heated to reflux at 80 °C for 2 h. After confirming the completion of the reaction by TLC, the solution was cooled to ambient temperature. The solvent was removed under reduced pressure, and then the residue was diluted with ethyl acetate (30 mL) and sequentially washed with saturated $NaHCO_3$ (20 mL × 2) and brine (15 mL), and dried over anhydrous Na_2SO_4. After the solution was filtered, the solvent was removed under reduced pressure, and the crude product was purified using silica gel flash column chromatography with a solvent mixture of ethyl acetate and hexane (2:1, *v*/*v*) for elution. The solvent of the corresponding fractions was evaporated under reduced pressure to give compound **9a** [19].

Ethyl 2-(3-(difluoromethyl)-1-methyl-1H-pyrazol-4-yl)thiazole-4-carboxylate (**9a**). Light yellow solid; yield, 83%; m.p.: 101–103 °C. ^{1}H NMR (400 MHz, $CDCl_3$) δ 8.04 (s, 1H), 7.97 (s, 1H), 6.96 (t, *J* = 53.9 Hz, 1H), 4.35 (q, *J* = 6.9 Hz, 2H), 3.89 (s, 3H), 1.34 (t, *J* = 6.5 Hz, 3H).^{13}C NMR (101 MHz, $CDCl_3$) δ 160.3, 157.7, 146.3, 141.8 (t, *J* = 27.5 Hz), 131.1, 125.9, 113.9, 109.8 (t, *J* = 234.7 Hz), 60.4, 38.5, 13.3. HRMS (ESI) *m*/*z* calcd for $C_{11}H_{11}F_2N_3NaO_2S$ $[M + Na]^+$: 310.0432; found: 310.0435.

4.1.4. Synthetic procedure for compound **9b**

The synthesis procedure was adjusted according to the procedure of **9a**. The ethyl bromopyruvate (1.07 mL, 6.85 mmol) was added dropwise to a solution of amide **2** (1.00 g, 5.71 mmol) in ethanol (20 mL) at room temperature. The solution was refluxed at 80 °C for 8 h. After confirming the completion of the reaction by TLC, the solution was cooled to room temperature. The solvent was removed, and the residue was diluted with ethyl acetate (20 mL) and sequentially washed with saturated $NaHCO_3$ (10 mL × 2) and brine (10 mL), and dried over anhydrous Na_2SO_4. Then the solution was filtered and concentrated under reduced pressure. The crude product was purified using silica gel flash column chromatography with a solvent mixture of ethyl acetate and hexane (2:1, *v*/*v*) for elution. The solvent of the corresponding fractions was evaporated under reduced pressure to yield compound **9b.**

Ethyl 2-(3-(difluoromethyl)-1-methyl-1H-pyrazol-4-yl)oxazole-4-carboxylate (**9b**). Yellow solid; yield, 35%; m.p.: 80–82 °C. ^{1}H NMR (400 MHz, $CDCl_3$) δ 8.23 (s, 1H), 8.08 (s, 1H), 7.13 (t, *J* = 53.7 Hz, 1H), 4.41 (q, *J* = 7.1 Hz, 2H), 4.00 (s, 3H), 1.40 (t, *J* = 7.1 Hz, 3H). ^{13}C NMR (101 MHz, $CDCl_3$) δ 161.1, 156.3, 143.7 (t, *J* = 26.3 Hz), 143.2, 134.3, 132.5, 109.8 (t, *J* = 236.2 Hz), 108.6, 61.4, 39.8, 14.3. HRMS (ESI) *m*/*z* calcd for $C_{11}H_{12}F_2N_3O_3$ $[M + H]^+$: 272.0841; found: 272.0841.

4.1.5. Synthetic procedure for compound **4**

Compound 4 was prepared according to a previously reported method with modifications [26]. Briefly, under an atmosphere of argon, compound **3** (5.00 g, 28.39 mmol) was suspended in 100 mL of tert-butanol. *N*, *N*-diisopropylethylamine (DIPEA, 9.89 mL, 56.78 mmol) and diphenyl phosphorazidate (DPPA, 10.16 g, 36.91 mmol) were added to the mixture with syringes. The resulting mixture was stirred for 10 min at 20 °C. Afterwards the mixture was stirred for 4 h at 80–90 °C. After confirmation of the completion of the reaction by TLC, the solution was cooled to room temperature, and the solvent was removed under reduced pressure. The residue was purified using silica gel flash column chromatography with a solvent mixture of ethyl acetate and hexane (4:1, *v*/*v*) for elution. The solvent of the corresponding fractions was evaporated under reduced pressure to afford compound **4**.

Tert-butyl (3-(difluoromethyl)-1-methyl-1H-pyrazol-4-yl)carbamate (**4**). White solid; yield, 94%; m.p.: 85–87 °C. ^{1}H NMR (400 MHz, $CDCl_3$) δ 7.86 (s, 1H), 6.70 (t, *J* = 54.6 Hz, 1H), 6.66 (s, 1H), 3.84 (s, 3H), 1.50 (s, 9H). ^{13}C NMR (101 MHz, $CDCl_3$) δ 152.6, 133.6 (t, *J* = 29.1 Hz), 122.5, 119.9, 112.6 (t, *J* = 231.5 Hz), 80.9, 39.4, 28.2.

4.1.6. Synthetic procedure for compound **5**

Compound **4** (6.31 g, 25.52 mmol) was dissolved in dichloromethane (50 mL). Trifluoroacetic acid (25 mL) was added dropwise and the mixture was allowed to stir at room temperature for 2.5 h. After confirmation of the completion of the reaction by TLC, the solvent was removed under reduced pressure. The residue was diluted with water (20 mL). The pH value of the solution was adjusted to 8 with saturated a $NaHCO_3$ solution. The solution was extracted with ethyl acetate, and then the combined organic layers were dried over anhydrous Na_2SO_4, filtered and concentrated under the reduced pressure. The residue was purified using silica gel flash column chromatography with a solvent mixture of ethyl acetate and hexane (2:1, *v*/*v*) for elution to afford the compound **5**.

3-(Difluoromethyl)-1-methyl-1H-pyrazol-4-amine (**5**). Brown liquid; yield, 96%. ^{1}H NMR (400 MHz, $CDCl_3$) δ 6.97 (s, 1H), 6.67 (t, J = 54.7 Hz, 1H), 3.77 (s, 3H), 3.30 (s, 2H).

4.1.7. Synthetic procedure for compound **6**

Compound **6** was synthesized according to a previously reported procedure [26]. Compound **5** (1.5 g, 10.20 mmol) was dissolved in a 4 mol/L HCl solution (76.5 mL) and cooled down to 0 °C. Afterwards sodium nitrite (0.91 g, 13.25 mmol) dissolved in water was added and the mixture was stirred for 1 h at 0 °C. Then potassium iodide (5.08 g, 30.59 mmol) was added portion-wise with vigorous stirring, and the mixture was warmed to 20 °C within 30 min. After confirmation of the completion of the reaction by TLC, the reaction mixture was neutralized with saturated a $NaHCO_3$ solution, extracted with dichloromethane (30 mL). The organic layer was sequentially washed with saturated $Na_2S_2O_3$ (20 mL × 2) and brine (10 mL), and extracted with dichloromethane (10 mL × 2). The combined organic layers were dried over anhydrous Na_2SO_4, filtered and concentrated under reduced pressure. The residue was purified by silica gel flash column chromatography with a solvent mixture of ethyl acetate and hexane (16:1, *v*/*v*) for elution to yield compound **6**.

3-(Difluoromethyl)-4-iodo-1-methyl-1H-pyrazole (**6**). Yellow liquid; yield, 58%. ^{1}H NMR (400 MHz, $CDCl_3$) δ 7.47 (s, 1H), 6.66 (t, *J* = 53.8 Hz, 1H), 3.92 (s, 3H). ^{13}C NMR (101 MHz, $CDCl_3$) δ146.4 (t, *J* = 26.8 Hz), 136.7, 111.1 (t, *J* = 235.1 Hz), 54.0 (t, *J* = 1.8 Hz), 39.7. HRMS (ESI) *m*/*z* calcd for $C_5H_6F_2IN_2$ $[M + H]^+$: 258.9538; found: 258.9540.

4.1.8. Synthetic procedure for compound **7**

The *n*-butyllithium (2.5 mol/L solution in hexane, 4.6 mL, 11.63 mmol) was added dropwise to a suspension of intermediate **6** (1.0 g, 3.88 mmol) in dry tetrahydrofuran (10 mL) via syringe at −78 °C under nitrogen. The resulting solution was stirred for 1 h at −78 °C. Then the isopropoxyboronic acid pinacol ester (2.16 g, 11.63 mmol) was added dropwise via syringe to the solution. The resulting mixture was stirred for 2 h. The reaction mixture was carefully quenched with water (10 mL) and extracted with ethyl acetate (10 mL × 2). The combined organic layers were washed with brine (10 mL) and extracted with ethyl acetate (5 mL × 2). The combined organic layers were dried over anhydrous Na_2SO_4, filtered and concentrated under reduced pressure. The residue was purified by silica gel flash column chromatography with a solvent mixture of ethyl acetate and hexane (8:1, *v*/*v*) for elution to afford product **7**.

3-(Difluoromethyl)-1-methyl-4-(4,4,5,5-tetramethyl-1,3,2-dioxaborolan-2-yl)-1H-pyrazole (**7**). White solid; yield, 68%; m.p.: 87–89 °C. ^{1}H NMR (400 MHz, $CDCl_3$) δ 7.66 (s, 1H), 6.96 (t, *J* = 54.4 Hz, 1H), 3.94 (s, 3H), 1.31 (s, 12H). ^{13}C NMR (101 MHz, $CDCl_3$) δ 151.3 (t, *J* = 23.8 Hz), 138.2, 110.5 (t, *J* = 235.2 Hz), 83.7, 39.1, 24.8. HRMS (ESI) *m*/*z* calcd for $C_{11}H_{18}BF_2N_2O_2$ $[M + H]^+$: 259.1424; found: 259.1436.

*4.1.9. Synthetic procedure for compound **9c***

Under a nitrogen atmosphere, compound **7** (0.5 g, 1.94 mmol), ethyl 5-bromothiophene-2-carboxylate (0.55 g, 2.32 mmol) and $Pd(PPh_3)_4$ (0.11 g, 0.05 mmol) were dissolved in THF (40 mL). 2 mol/L Na_2CO_3 (1.94 mL, 3.87 mmol) was added and the mixture was stirred overnight at 100 °C. After confirmation of the completion of the reaction by TLC, the solution was cooled to room temperature, the precipitate was removed by filtering through a pad of celite and washed with ethyl acetate. The filtrate was concentrated under reduced pressure. The residue was purified by silica gel flash column chromatography with a solvent mixture of ethyl acetate and hexane (8:1, *v*/*v*) for elution to afford the compound **9c**.

*Ethyl 5-(3-(difluoromethyl)-1-methyl-1H-pyrazol-*4-yl*)thiophene-2-carboxylate* (**9c**). Yellow solid; yield, 74%; m.p.: 56–58 °C. ^{1}H NMR (400 MHz, $CDCl_3$) δ 7.72 (d, *J* = 3.8 Hz, 1H), 7.61 (s, 1H), 7.20 (d, *J* = 3.8 Hz, 1H), 6.76 (t, *J* = 53.9 Hz, 1H), 4.35 (q, *J* = 7.1 Hz, 2H), 3.95 (s, 3H), 1.38 (t, *J* = 7.1 Hz, 3H). ^{13}C NMR (101 MHz, $CDCl_3$) δ 162.2, 142.3 (t, *J* = 28.3 Hz), 139.1, 134.1, 132.4, 130.7, 126.4, 114.5, 111.4 (t, *J* = 234.2 Hz), 61.2, 39.4, 14.4. HRMS (ESI) *m*/*z* calcd for $C_{12}H_{13}F_2N_2O_2S$ $[M + H]^+$: 287.0660; found: 287.0664.

*4.1.10. General procedure for compounds **9d-9e***

Compound **8** (1 equiv.), corresponding boronic acid (1.2 equiv.), Cs_2CO_3 (2 equiv.), $PdCl_2$(dppf) (0.05 equiv.) were dissolved in a mixed solution of dioxane/H_2O (10:1, *v*/*v*) under a nitrogen atmosphere. The reaction mixture was heated to reflux overnight at 110 °C. After confirmation of the completion of the reaction by TLC, the solution was cooled to room temperature. The mixture was filtered through a pad of celite and the filtrate was concentrated under reduced pressure. The residue was purified by silica gel flash column chromatography with a solvent mixture of ethyl acetate and hexane (8:1, *v*/*v*) for elution to afford compounds **9d-9e** (63-89%).

*Ethyl 4-(3-(difluoromethyl)-1-methyl-1H-pyrazol-*4-yl*)benzoate* (**9d**). White solid; yield, 65%; m.p.: 139–141 °C. ^{1}H NMR (400 MHz, $CDCl_3$) δ 7.97 (d, *J* = 8.1 Hz, 2H), 7.48 (d, *J* = 2.9 Hz, 2H), 7.45 (s, 1H), 6.72 (t, *J* = 54.1 Hz, 1H), 4.29 (q, *J* = 7.0 Hz, 2H), 3.81 (s, 3H), 1.31 (t, *J* = 7.1 Hz, 3H). ^{13}C NMR (101 MHz, $CDCl_3$) δ 166.2, 142.2 (t, *J* = 27.8 Hz), 135.7, 130.7, 129.8, 129.0, 127.8, 120.9, 111.9 (t, *J* = 233.8 Hz), 60.9, 39.1, 14.2. HRMS (ESI) *m*/*z* calcd for $C_{14}H_{15}F_2N_2O_2$ $[M + H]^+$: 281.1096; found: 281.1096.

*Ethyl 3-(3-(difluoromethyl)-1-methyl-1H-pyrazol-*4-yl*)benzoate* (**9ea**). Yellow oil; yield, 63%. ^{1}H NMR (400 MHz, $CDCl_3$) δ 8.13 (s, 1H), 7.97 (d, *J* = 7.8 Hz, 1H), 7.68 (d, *J* = 7.7 Hz, 1H), 7.56 (s, 1H), 7.45 (t, *J* = 7.7 Hz, 1H), 6.76 (t, *J* = 54.1 Hz, 1H), 4.37 (q, *J* = 7.1 Hz, 2H), 3.93 (s, 3H), 1.39 (t, *J* = 7.1 Hz, 3H). ^{13}C NMR (101 MHz, $CDCl_3$) δ 166.4, 142.3 (t, *J* = 27.6 Hz), 132.6 (t, *J* = 2.1 Hz), 131.5, 130.9, 130.6, 129.1, 128.7, 128.2, 121.2, 111.8 (t, *J* = 233.9 Hz), 39.3, 14.3. HRMS (ESI) *m*/*z* calcd for $C_{14}H_{15}F_2N_2O_2$ $[M + H]^+$: 281.1096; found: 281.1102.

*Ethyl 3-(1-methyl-3-(trifluoromethyl)-1H-pyrazol-*4-yl*)benzoate* (**9eb**). Yellow oil; yield, 89%. ^{1}H NMR (400 MHz, $CDCl_3$) δ 8.07 (s, 1H), 8.02 (d, *J* = 7.7 Hz, 1H), 7.60 (d, *J* = 7.6 Hz, 1H), 7.55 (s, 1H), 7.46 (t, *J* = 7.7 Hz, 1H), 4.39 (q, *J* = 7.1 Hz, 2H), 3.99 (s, 3H), 1.40 (t, *J* = 7.1 Hz, 3H). ^{13}C NMR (101 MHz, $CDCl_3$) δ 166.3, 138.5 (q, *J* = 36.5 Hz), 132.9, 131.1, 130.9, 129.6, 128.7, 128.6, 121.5 (q, *J* = 269.2 Hz), 121.5, 61.1, 39.6, 14.3. HRMS (ESI) *m*/*z* calcd for $C_{14}H_{14}F_3N_2O_2$ $[M + H]^+$: 299.1002; found: 299.1006.

*Ethyl 3-(1,3-dimethyl-1H-pyrazol-*4-yl*)benzoate* (**9ec**). Yellow oil; yield, 86%. ^{1}H NMR (400 MHz, $CDCl_3$) δ 8.06 (s, 1H), 7.92 (d, *J* = 7.7 Hz, 1H), 7.57 (d, *J* = 7.7 Hz, 1H), 7.49 (s, 1H), 7.44 (t, *J* = 7.7 Hz, 1H), 4.39 (q, *J* = 7.1 Hz, 2H), 3.89 (s, 3H), 2.41 (s, 3H), 1.41 (t, *J* = 7.1 Hz, 3H). ^{13}C NMR (101 MHz, $CDCl_3$) δ 166.6, 145.7, 133.9, 131.6, 130.9, 129.1, 128.6, 128.4, 127.1, 120.2, 61.0, 38.7, 14.4, 13.2. HRMS (ESI) *m*/*z* calcd for $C_{14}H_{17}N_2O_2$ $[M + H]^+$: 245.1285; found: 245.1284.

*4.1.11. General procedure for compounds **10a-10e***

According to the procedure previously reported [27], the intermediates **9a-9e** (1 equiv.) were dissolved in a mixed solution of 2 mol/L NaOH/EtOH (4:1, *v*/*v*) and heated to reflux for 30 min at 80 °C. After completion of the reaction, the solution was cooled to room temperature, then acidified to pH = 2 with a 2 mol/L HCl solution. The precipitated solid was filtered and dried to give the corresponding carboxylic acids **10a-10e** (56–93%).

*2-(3-(Difluoromethyl)-1-methyl-1H-pyrazol-*4-yl*)thiazole-4-carboxylic acid* (**10a**) [19]. Off-white solid; yield, 91%; m.p.: 213–215 °C. ^{1}H NMR (400 MHz, DMSO-d_6) δ 13.14 (s, 1H), 8.59 (s, 1H), 8.45 (s, 1H), 7.41 (t, *J* = 53.6 Hz, 1H), 3.98 (s, 3H). ^{13}C NMR (101 MHz, DMSO-d_6) δ 162.3, 158.8, 147.9, 141.9 (t, *J* = 25.4 Hz), 133.6, 128.5, 114.5, 111.0 (t, *J* = 233.5 Hz), 39.8. HRMS (ESI) *m*/*z* calcd for $C_9H_7F_2N_3NaO_2S$ $[M + Na]^+$: 282.0119; found: 282.0122.

*2-(3-(Difluoromethyl)-1-methyl-1H-pyrazol-*4-yl*)oxazole-4-carboxylic acid* (**10b**). Yellow solid; yield, 56%; m.p.: 224–226 °C. ^{1}H NMR (400 MHz, DMSO) δ 13.19 (s, 1H), 8.80 (d, *J* = 2.7 Hz, 1H), 8.56 (d, *J* = 2.9 Hz, 1H), 7.30 (t, *J* = 53.5 Hz, 1H), 3.97 (s, 3H). ^{13}C NMR (101 MHz, DMSO) δ 162.4, 156.0, 145.1, 142.7 (t, *J* = 25.5 Hz), 134.5, 133.9, 110.4 (t, *J* = 234.2 Hz), 108.0 (t, *J* = 2.8 Hz), 39.8. HRMS (ESI) *m*/*z* calcd for $C_9H_8F_2N_3O_3$ $[M + H]^+$: 244.0528; found: 244.0531.

*5-(3-(Difluoromethyl)-1-methyl-1H-pyrazol-*4-yl*)thiophene-2-carboxylic acid* (**10c**). Yellow solid; yield, 79%; m.p.: 185–187 °C. ^{1}H NMR (400 MHz, DMSO) δ 13.14 (s, 1H), 8.32 (s, 1H), 7.73–7.67 (m, 1H), 7.24–7.22 (m, 1H), 7.12 (t, *J* = 53.2 Hz, 1H), 3.92 (s, 3H). ^{13}C NMR (101 MHz, DMSO) δ 163.2, 141.3 (t, *J* = 28.0 Hz), 139.5, 134.4, 133.2, 132.9, 126.4, 113.4, 112.2 (t, *J* = 231.9 Hz), 39.3. HRMS (ESI) *m*/*z* calcd for $C_{10}H_9F_2N_2O_2S$ $[M + H]^+$: 259.0347; found: 259.0352.

*4-(3-(Difluoromethyl)-1-methyl-1H-pyrazol-*4-yl*)benzoic acid* (**10d**). White solid; yield, 91%; m.p.: 194–196 °C. ^{1}H NMR (400 MHz, DMSO) δ 12.96 (s, 1H), 8.26 (s, 1H), 7.97 (d, *J* = 8.2 Hz, 2H), 7.62 (d, *J* = 8.3 Hz, 2H), 7.11 (t, *J* = 53.6 Hz, 1H), 3.93 (s, 3H). ^{13}C NMR (101 MHz, DMSO) δ 167.0, 141.2 (t, *J* = 27.7 Hz), 135.6, 132.3, 129.7, 129.0, 127.5, 119.6, 112.0 (t, *J* = 232.1 Hz), 39.3. HRMS (ESI) *m*/*z* calcd for $C_{12}H_{11}F_2N_2O_2$ $[M + H]^+$: 253.0783; found: 253.0786.

*3-(3-(Difluoromethyl)-1-methyl-1H-pyrazol-*4-yl*)benzoic acid* (**10ea**). White solid; yield, 87%; m.p.: 141–142 °C. ^{1}H NMR (400 MHz, DMSO) δ 13.06 (s, 1H), 8.24 (s, 1H), 8.10 (s, 1H), 7.88 (d, *J* = 7.6 Hz, 1H), 7.73 (d, *J* = 7.6 Hz, 1H), 7.55 (t, *J* = 7.7 Hz, 1H), 7.07 (t, *J* = 53.7 Hz, 1H), 3.93 (s, 3H). ^{13}C NMR (101 MHz, DMSO) δ 167.1, 141.0 (t, *J* = 27.6 Hz), 132.0, 131.8, 131.6, 131.3, 129.0, 128.4, 127.7, 119.7, 112.2 (t, *J* = 231.6 Hz), 39.3. HRMS (ESI) *m*/*z* calcd for $C_{12}H_{11}F_2N_2O_2$ $[M + H]^+$: 253.0783; found: 253.0787.

*3-(1-Methyl-3-(trifluoromethyl)-1H-pyrazol-*4-yl*)benzoic acid* (**10eb**). White solid; yield, 93%; m.p.: 162–164 °C. ^{1}H NMR (400 MHz, DMSO) δ 13.15 (s, 1H), 8.27 (s, 1H), 8.02 (s, 1H), 7.95 (d, *J* = 7.6 Hz, 1H), 7.66 (d, *J* = 7.6 Hz, 1H), 7.58 (t, *J* = 7.5 Hz, 1H), 3.98 (s, 3H). ^{13}C NMR (101 MHz, DMSO) δ 167.0, 136.2 (q, *J* = 35.5 Hz), 132.9, 132.3, 131.2, 130.7, 129.0, 128.7, 128.3, 121.8 (q, *J* = 268.9 Hz), 120.1, 39.3. HRMS (ESI) *m*/*z* calcd for $C_{12}H_{10}F_3N_2O_2$ $[M + H]^+$: 271.0689; found: 271.0688.

*3-(1,3-Dimethyl-1H-pyrazol-*4-yl*)benzoic acid* (**10ec**). White solid; yield: 92%; m.p.: 183–185 °C; ^{1}H NMR (400 MHz, DMSO) δ 13.03 (s, 1H), 8.01–7.98 (m, 2H), 7.83–7.79 (m, 1H), 7.67 (d, *J* = 7.7 Hz, 1H), 7.51 (t, *J* = 7.7 Hz, 1H), 3.80 (s, 3H), 2.32 (s, 3H). ^{13}C NMR (101 MHz, DMSO) δ 167.8, 144.5, 134.4, 131.7, 131.3, 130.4, 129.4, 127.7, 127.0, 119.2, 38.7, 13.7. HRMS (ESI) *m*/*z* calcd for $C_{12}H_{13}N_2O_2$ $[M + H]^+$: 217.0972; found: 217.0975.

*4.1.12. General procedure for target compounds **11aa-11eh***

The carboxylic acids **10a-10e** (1 equiv.) were dissolved in dichloromethane, *N*, *N*-diisopropylethylamine (DIPEA, 2 equiv.) and Benzotriazol-1-yl- oxytripyrrolidinophosphonium hexafluorophosphate (PyBOP, 1.1 equiv.) were added at 0 °C. After

15 min, the corresponding amine (1.2 equiv.) was added. And then, the reaction mixture was stirred overnight at room temperature. The completion of the reaction was monitored by TLC, the solution was sequentially washed with water and brine, and extracted with dichloromethane. The combined organic layers were dried over anhydrous Na_2SO_4, then filtered and concentrated under reduced pressure. The crude residues were purified by silica gel column chromatography to afford title compounds **11aa-11eh** (30–99%).

*N-(2-chlorophenyl)-2-(3-(difluoromethyl)-1-methyl-1H-pyrazol-*4-yl*)thiazole-4-carboxamide* (**11aa**). White solid; yield: 50%; purity: 100%; m.p.: 177–178 °C; ^{1}H NMR (400 MHz, $CDCl_3$) δ 9.93 (s, 1H), 8.61 (d, *J* = 8.2 Hz, 1H), 8.15 (s, 1H), 7.93 (s, 1H), 7.43 (dd, *J* = 8.0, 0.8 Hz, 1H), 7.33 (t, *J* = 7.8 Hz, 1H), 7.16 (t, *J* = 53.9 Hz, 2H), 7.11–7.02 (m, 1H), 4.01 (s, 3H). ^{13}C NMR (101 MHz, $CDCl_3$) δ 158.6, 158.5, 150.2, 143.1 (t, *J* = 26.6 Hz), 134.7, 131.5, 129.2, 127.8, 124.7, 123.3, 123.0, 120.9, 114.9, 110.4 (t, *J* = 235.9 Hz), 39.7. HRMS (ESI) *m*/*z* calcd for $C_{15}H_{12}ClF_2N_4OS$ $[M + H]^+$: 369.0383; found: 369.0383.

*N-(3-chlorophenyl)-2-(3-(difluoromethyl)-1-methyl-1H-pyrazol-*4-yl*)thiazole-4-carboxamide* (**11 ab**). White solid; yield: 87%; purity: 100%; m.p.: 141–143 °C; ^{1}H NMR (400 MHz, $CDCl_3$) δ 9.22 (s, 1H), 8.14 (s, 1H), 7.95 (s, 1H), 7.82 (t, *J* = 1.9 Hz, 1H), 7.53 (dd, *J* = 8.1, 1.2 Hz, 1H), 7.29 (t, *J* = 8.1 Hz, 1H), 7.12 (d, *J* = 8.1 Hz, 1H), 6.99 (t, *J* = 49.2 Hz, 1H), 4.00 (s, 3H). ^{13}C NMR (101 MHz, $CDCl_3$) δ 158.6, 158.3, 149.9, 142.9 (t, *J* = 27.7 Hz), 138.8, 134.8, 131.7, 130.1, 124.5, 123.6, 119.7, 117.7, 114.8, 110.8 (t, *J* = 235.3 Hz), 39.7. HRMS (ESI) *m*/*z* calcd for $C_{15}H_{11}ClF_2N_4NaOS$ $[M + Na]^+$: 391.0202; found: 391.0206.

*N-(4-chlorophenyl)-2-(3-(difluoromethyl)-1-methyl-1H-pyrazol-*4-yl*)thiazole-4-carboxamide* (**11ac**). Yellow solid; yield: 73%; purity: 99%; m.p.: 179–180 °C; ^{1}H NMR (400 MHz, $CDCl_3$) δ 9.20 (s, 1H), 8.11 (s, 1H), 7.93 (s, 1H), 7.64 (d, *J* = 8.3 Hz, 2H), 7.32 (d, *J* = 8.3 Hz, 2H), 7.00 (t, *J* = 53.8 Hz, 1H), 3.99 (s, 3H). ^{13}C NMR (101 MHz, $CDCl_3$) δ 158.6, 158.3, 149.9, 142.9 (t, *J* = 27.5 Hz), 136.3, 131.7, 129.3, 129.1, 123.4, 120.9, 114.7, 110.8 (t, *J* = 235.3 Hz), 39.6. HRMS (ESI) *m*/*z* calcd for $C_{15}H_{11}ClF_2N_4NaOS$ $[M + Na]^+$: 391.0202; found: 391.0205.

*2-(3-(Difluoromethyl)-1-methyl-1H-pyrazol-*4-yl*)-N-(2-methoxyphenyl)thiazole-4-carboxamide* (**11ad**). White solid; yield: 84%; purity: 100%; m.p.: 194–196 °C; ^{1}H NMR (400 MHz, $CDCl_3$) δ 9.97 (s, 1H), 8.53 (dd, *J* = 7.9, 1.5 Hz, 1H), 8.06 (s, 1H), 7.85 (s, 1H), 7.30 (t, *J* = 53.9 Hz, 1H), 7.08 (td, *J* = 7.8, 1.6 Hz, 1H), 7.00 (td, *J* = 7.7, 1.1 Hz, 1H), 6.92 (dd, *J* = 8.0, 1.0 Hz, 1H), 3.98 (s, 3H), 3.97 (s, 3H). ^{13}C NMR (101 MHz, $CDCl_3$) δ 158.3, 158.2, 150.8, 148.3, 143.1 (t, *J* = 25.3 Hz), 131.1, 127.6, 124.0, 122.2, 121.1, 119.3, 115.1, 110.2 (t, *J* = 236.1 Hz), 110.0, 55.8, 39.7. HRMS (ESI) *m*/*z* calcd for $C_{16}H_{14}F_2N_4NaO_2S$ $[M + Na]^+$: 387.0698; found: 387.0702.

*2-(3-(Difluoromethyl)-1-methyl-1H-pyrazol-*4-yl*)-N-(3-methoxyphenyl)thiazole-4-carboxamide* (**11ae**). Light yellow solid; yield: 98%; purity: 100%; m.p.: 165–167 °C; ^{1}H NMR (400 MHz, $CDCl_3$) δ 9.20 (s, 1H), 8.12 (s, 1H), 7.94 (s, 1H), 7.50 (t, *J* = 2.1 Hz, 1H), 7.26 (t, *J* = 8.1 Hz, 1H), 7.14 (dd, *J* = 7.6, 1.4 Hz, 1H), 7.01 (t, *J* = 53.9 Hz, 1H), 6.71 (dd, *J* = 8.2, 1.9 Hz, 1H), 3.99 (s, 3H), 3.84 (s, 3H). ^{13}C NMR (101 MHz, $CDCl_3$) δ 160.3, 158.6, 158.2, 150.3, 142.9 (t, *J* = 27.6 Hz), 138.9, 131.7, 129.8, 123.2, 114.8, 111.9, 110.8 (t, *J* = 235.4 Hz), 110.4, 105.3, 55.4, 39.6. HRMS (ESI) *m*/*z* calcd for $C_{16}H_{14}F_2N_4NaO_2S$ $[M + Na]^+$: 387.0703; found: 387.0702.

*2-(3-(Difluoromethyl)-1-methyl-1H-pyrazol-*4-yl*)-N-(4-methoxyphenyl)thiazole-4-carboxamide* (**11af**). Yellow solid; yield: 99%; purity: 100%; m.p.: 170–172 °C; ^{1}H NMR (400 MHz, $CDCl_3$) δ 9.11 (s, 1H), 8.12 (s, 1H), 7.95 (s, 1H), 7.62 (d, *J* = 8.9 Hz, 2H), 7.03 (t, *J* = 53.8 Hz, 1H), 6.92 (d, *J* = 8.9 Hz, 2H), 4.01 (s, 3H), 3.82 (s, 3H). ^{13}C NMR (101 MHz, $CDCl_3$) δ 158.4, 158.1, 156.5, 150.4, 142.9 (t, *J* = 27.4 Hz), 131.7, 130.8, 122.9, 121.4, 114.9, 114.3, 110.7 (t, *J* = 235.3 Hz), 55.5, 39.7. HRMS (ESI) *m*/*z* calcd for $C_{16}H_{14}F_2N_4NaO_2S$ $[M + Na]^+$: 387.0698; found: 387.0702.

*2-(3-(Difluoromethyl)-1-methyl-1H-pyrazol-*4-yl*)-N-(2-(trifluoromethoxy)phenyl) thiazole-4-carboxamide* (**11 ag**). Yellow solid; yield: 30%; purity: 100%; m.p.: 140–142 °C; ^{1}H NMR (400 MHz, $CDCl_3$) δ 9.71 (s, 1H), 8.65 (d, *J* = 8.1 Hz, 1H), 8.16 (s, 1H), 7.92 (s, 1H), 7.34 (dd, *J* = 14.3, 7.3 Hz, 2H), 7.15 (t, *J* = 7.7 Hz, 1H), 7.10 (t, *J* = 53.9 Hz, 1H), 4.01 (s, 3H). ^{13}C NMR (101 MHz, $CDCl_3$) δ 158.6, 158.6, 150.0, 143.0 (t, *J* = 26.8 Hz), 138.2, 131.6, 130.7, 127.7, 124.2, 123.5, 121.2, 120.7 (q, *J* = 258.8 Hz), 120.6, 114.9, 110.4 (t, *J* = 235.7 Hz), 39.7. HRMS (ESI) *m*/*z* calcd for $C_{16}H_{12}F_5N_4O_2S$ $[M + H]^+$: 419.0596; found: 419.0596.

*2-(3-(Difluoromethyl)-1-methyl-1H-pyrazol-*4-yl*)-N-(3-(trifluoromethoxy)phenyl) thiazole-4-carboxamide* (**11ah**). White solid; yield: 90%; purity: 100%; m.p.: 139–141 °C; ^{1}H NMR (400 MHz, $CDCl_3$) δ 9.29 (s, 1H), 8.16 (s, 1H), 7.97 (s, 1H), 7.78 (s, 1H), 7.53 (dd, *J* = 8.2, 1.2 Hz, 1H), 7.38 (t, *J* = 8.2 Hz, 1H), 7.14–6.99 (m, 1H), 6.99 (t, *J* = 53.8 Hz, 1H), 4.02 (s, 3H). ^{13}C NMR (101 MHz, $CDCl_3$) δ 158.7, 158.3, 149.8, 149.7, 143.0 (t, *J* = 27.9 Hz), 139.1, 131.8, 130.1, 123.7, 121.8, 117.7, 116.5, 114.7, 112.5, 110.8 (t, *J* = 235.3 Hz), 39.7. HRMS (ESI) *m*/*z* calcd for $C_{16}H_{12}F_5N_4O_2S$ $[M + H]^+$: 419.0596; found: 419.0595.

*2-(3-(Difluoromethyl)-1-methyl-1H-pyrazol-*4-yl*)-N-(4-(trifluoromethoxy)phenyl) thiazole-4-carboxamide* (**11ai**). White solid; yield: 93%; purity: 100%; m.p.: 151–153 °C; ^{1}H NMR (400 MHz, $CDCl_3$) δ 9.27 (s, 1H), 8.15 (s, 1H), 7.95 (s, 1H), 7.74 (d, *J* = 9.0 Hz, 2H), 7.23 (d, *J* = 8.6 Hz, 2H), 7.00 (t, *J* = 53.8 Hz, 1H), 4.01 (s, 3H). ^{13}C NMR (101 MHz, $CDCl_3$) δ 158.6, 158.3, 149.9, 145.4, 143.0 (t, *J* = 27.7 Hz), 136.3, 131.7, 123.5, 121.9, 120.8, 119.2, 114.8, 110.8 (t, *J* = 235.3 Hz), 39.7. HRMS (ESI) *m*/*z* calcd for $C_{16}H_{11}F_5N_4NaO_2S$ $[M + Na]^+$: 441.0415; found: 441.0418.

*2-(3-(Difluoromethyl)-1-methyl-1H-pyrazol-*4-yl*)-N-(2-isopropylphenyl)thiazole-4-carboxamide* (**11aj**). Yellow solid; yield: 87%; purity: 100%; m.p.: 109–111 °C; ^{1}H NMR (400 MHz, $CDCl_3$) δ 9.38 (s, 1H), 8.20 (d, *J* = 7.9 Hz, 1H), 8.12 (s, 1H), 7.88 (s, 1H), 7.33 (d, *J* = 7.5 Hz, 1H), 7.25 (d, *J* = 7.9 Hz, 1H), 7.18 (t, *J* = 7.3 Hz, 1H), 7.11 (t, *J* = 53.9 Hz, 1H), 3.97 (s, 3H), 3.20 (dt, *J* = 13.5, 6.7 Hz, 1H), 1.34 (d, *J* = 6.8 Hz, 6H). ^{13}C NMR (101 MHz, $CDCl_3$) δ 158.7, 158.4, 150.8, 142.8 (t, *J* = 26.6 Hz), 138.6, 134.3, 131.6, 126.5, 125.6, 125.3, 122.8, 122.4, 115.0, 110.4 (t, *J* = 235.8 Hz), 39.7, 28.0, 22.9. HRMS (ESI) *m*/*z* calcd for $C_{18}H_{19}F_2N_4OS$ $[M + H]^+$: 377.1242; found: 377.1249.

*N-(3,5-dibromophenyl)-2-(3-(difluoromethyl)-1-methyl-1H-pyrazol-*4-yl*)thiazole-4-carboxamide* (**11ak**). Yellow solid; yield: 64%; purity: 100%; m.p.: 154–156 °C; ^{1}H NMR (400 MHz, $CDCl_3$) δ 9.21 (s, 1H), 8.17 (s, 1H), 7.98 (s, 1H), 7.87 (d, *J* = 1.4 Hz, 2H), 7.44 (s, 1H), 6.98 (t, *J* = 53.8 Hz, 1H), 4.02 (s, 3H). ^{13}C NMR (101 MHz, $CDCl_3$) δ 158.6, 158.5, 149.4, 143.0 (t, *J* = 26.1 Hz), 139.8, 131.8, 129.8, 124.0, 123.1, 121.1, 114.6, 110.9 (t, *J* = 235.3 Hz), 39.7. HRMS (ESI) *m*/*z* calcd for $C_{15}H_{11}Br_2F_2N_4OS$ $[M + H]^+$: 490.8983; found: 490.8973.

*N-(3,4-dichlorophenyl)-2-(3-(difluoromethyl)-1-methyl-1H-pyrazol-*4-yl*)thiazole-4-carboxamide* (**11 al**). White solid; yield: 88%; purity: 99%; m.p.: 173–175 °C; ^{1}H NMR (400 MHz, $CDCl_3$) δ 9.23 (s, 1H), 8.15 (s, 1H), 7.96 (s, 1H), 7.95 (d, *J* = 2.5 Hz, 1H), 7.52 (dd, *J* = 8.7, 2.5 Hz, 1H), 7.42 (d, *J* = 8.7 Hz, 1H), 6.99 (t, *J* = 53.8 Hz, 1H), 4.02 (s, 3H). ^{13}C NMR (101 MHz, $CDCl_3$) δ 157.6, 157.4, 148.5, 141.9 (t, *J* = 27.9 Hz), 136.1, 131.9, 130.7, 129.6, 126.5, 122.8, 120.2, 117.9, 113.6, 109.8 (t, *J* = 235.2 Hz), 38.7. HRMS (ESI) *m*/*z* calcd for $C_{15}H_{11}Cl_2F_2N_4OS$ $[M + H]^+$: 402.9993; found: 402.9993.

*N-(3,5-dichlorophenyl)-2-(3-(difluoromethyl)-1-methyl-1H-pyrazol-*4-yl*)thiazole-4-carboxamide* (**11am**). Light yellow solid; yield: 58%; purity: 100%; m.p.: 181–183 °C; ^{1}H NMR (400 MHz, $CDCl_3$) δ 9.22 (s, 1H), 8.14 (s, 1H), 7.95 (s, 1H), 7.66 (d, *J* = 1.6 Hz, 2H), 7.12 (t, *J* = 1.6 Hz, 1H), 6.97 (t, *J* = 53.8 Hz, 1H), 4.00 (s, 3H). ^{13}C NMR (101 MHz, $CDCl_3$) δ 158.6, 158.5, 149.4, 143.0 (t, *J* = 27.9 Hz), 139.5, 135.4, 131.8, 124.3, 124.0, 117.9, 114.6, 110.9 (t, *J* = 235.2 Hz), 39.7. HRMS (ESI) *m*/*z* calcd for $C_{15}H_{11}Cl_2F_2N_4OS$ $[M + H]^+$: 402.9993; found: 402.9996.

*N-cyclopropyl-2-(3-(difluoromethyl)-1-methyl-1H-pyrazol-*4-yl*) thiazole-4-carboxamide* (**11an**). White solid; yield: 96%; purity:

100%; m.p.: 116–118 °C; ^{1}H NMR (400 MHz, $CDCl_3$) δ 8.06 (s, 1H), 7.91 (s, 1H), 7.34 (s, 1H), 7.00 (t, J = 53.9 Hz, 1H), 4.00 (s, 3H), 2.92 (tq, J = 7.3, 3.7 Hz, 1H), 0.94–0.86 (m, 2H), 0.70–0.63 (m, 2H). ^{13}C NMR (101 MHz, $CDCl_3$) δ 162.2, 158.1, 150.2, 142.9 (t, J = 27.0 Hz), 131.5, 122.5, 115.0, 110.6 (t, J = 235.3 Hz), 39.6, 22.5, 6.8. HRMS (ESI) m/z calcd for $C_{12}H_{13}F_2N_4OS$ $[M + H]^+$: 299.0773; found: 299.0774.

N-cyclohexyl-2-(3-(difluoromethyl)-1-methyl-1H-pyrazol-4-yl*) thiazole-4-carboxamide* (**11ao**). Light yellow solid; yield: 99%; purity: 100%; m.p.: 115–117 °C; ^{1}H NMR (400 MHz, $CDCl_3$) δ 8.03 (s, 1H), 7.93 (s, 1H), 7.24 (d, J = 8.1 Hz, 1H), 7.02 (t, J = 53.9 Hz, 1H), 3.99 (s, 3H), 2.05–1.97 (m, 2H), 1.80–1.71 (m, 2H), 1.68–1.60 (m, 1H), 1.50–1.38 (m, 2H), 1.37–1.19 (m, 4H). ^{13}C NMR (101 MHz, $CDCl_3$) δ 159.9, 157.9, 150.7, 142.8 (t, J = 27.0 Hz), 131.6, 122.3, 115.1, 110.6 (t, J = 235.3 Hz), 48.0, 39.6, 33.0, 25.6, 24.7. HRMS (ESI) m/z calcd for $C_{15}H_{18}F_2N_4NaOS$ $[M + Na]^+$: 363.1062; found: 363.1062.

2-(3-(Difluoromethyl)-1-methyl-1H-pyrazol-4-yl*)-N-(naphthalen*-1-yl*)thiazole-4-carboxamide* (**11ap**). White solid; yield: 72%; purity: 99%; m.p.: 172–174 °C; ^{1}H NMR (400 MHz, $CDCl_3$) δ 9.37 (s, 1H), 8.41 (s, 1H), 8.16 (s, 1H), 7.93 (s, 1H), 7.88–7.77 (m, 3H), 7.63 (d, J = 7.9 Hz, 1H), 7.45 (dd, J = 18.3, 7.1 Hz, 2H), 7.05 (t, J = 54.0 Hz, 1H), 3.98 (s, 3H). ^{13}C NMR (101 MHz, $CDCl_3$) δ 158.8, 158.2, 150.3, 142.9 (t, J = 27.4 Hz), 135.1, 133.9, 131.7, 130.7, 128.9, 127.8, 127.6, 126.6, 125.1, 123.3, 119.7, 116.4, 114.9, 110.8 (t, J = 235.3 Hz), 39.6. HRMS (ESI) m/z calcd for $C_{19}H_{15}F_2N_4OS$ $[M + H]^+$: 385.0929; found: 385.0931.

2-(3-(Difluoromethyl)-1-methyl-1H-pyrazol-4-yl*)-N-(1,2,3,4-tetrahydronaphthalen*-1-yl*)thiazole-4-carboxamide* (**11aq**). Green solid; yield: 80%; purity: 100%; m.p.: 136–138 °C; ^{1}H NMR (400 MHz, $CDCl_3$) δ 8.11 (s, 1H), 7.90 (s, 1H), 7.56 (d, J = 8.9 Hz, 1H), 7.39–7.35 (m, 1H), 7.23–7.12 (m, 3H), 6.92 (t, J = 53.9 Hz, 1H), 5.39 (dd, J = 14.6, 5.8 Hz, 1H), 3.96 (s, 3H), 2.94–2.77 (m, 2H), 2.23–2.13 (m, 1H), 1.97–1.87 (m, 3H). ^{13}C NMR (101 MHz, $CDCl_3$) δ 160.3, 158.1, 150.3, 142.8 (t, J = 27.5 Hz), 137.6, 136.7, 131.7, 129.2, 128.7, 127.3, 126.3, 122.9, 115.0, 110.7 (t, J = 235.2 Hz), 47.5, 39.6, 30.4, 29.3, 20.3. HRMS (ESI) m/z calcd for $C_{19}H_{19}F_2N_4OS$ $[M + H]^+$: 389.1242; found: 389.1242.

2-(3-(Difluoromethyl)-1-methyl-1H-pyrazol-4-yl*)-N-(5,6,7,8-tetrahydronaphthalen*-2-yl*)thiazole-4-carboxamide* (**11ar**). White solid; yield: 95%; purity: 99%; m.p.: 188–190 °C; ^{1}H NMR (400 MHz, $CDCl_3$) δ 9.27 (s, 1H), 8.13 (s, 1H), 8.10 (d, J = 8.0 Hz, 1H), 7.90 (s, 1H), 7.18 (t, J = 7.8 Hz, 1H), 7.08 (t, J = 53.9 Hz, 1H), 6.93 (d, J = 7.6 Hz, 1H), 4.02 (s, 3H), 2.78 (dt, J = 20.7, 6.3 Hz, 4H), 1.97–1.87 (m, 2H), 1.85–1.76 (m, 2H). ^{13}C NMR (101 MHz, $CDCl_3$) δ 158.4, 158.1, 150.9, 142.9 (d, J = 26.9 Hz), 138.1, 135.4, 131.5, 126.8, 125.9, 125.7, 122.7, 118.5, 115.0, 110.5 (t, J = 235.7 Hz), 39.7, 29.9, 24.1, 22.9, 22.5. HRMS (ESI) m/z calcd for $C_{19}H_{19}F_2N_4OS$ $[M + H]^+$: 389.1242; found: 389.1244.

2-(3-(Difluoromethyl)-1-methyl-1H-pyrazol-4-yl*)-N-(pyridin*-2-yl*)thiazole-4-carboxamide* (**11as**). Yellow solid; yield: 99%; purity: 100%; m.p.: 115–117 °C; ^{1}H NMR (400 MHz, $CDCl_3$) δ 9.76 (s, 1H), 8.38 (d, J = 4.7 Hz, 1H), 8.31 (d, J = 8.3 Hz, 1H), 8.19 (s, 1H), 8.09 (s, 1H), 7.80–7.73 (m, 1H), 7.09 (dd, J = 7.2, 5.1 Hz, 1H), 6.99 (t, J = 53.8 Hz, 1H), 4.01 (s, 3H). ^{13}C NMR (101 MHz, $CDCl_3$) δ 159.1, 158.6, 151.0, 149.5, 148.1, 142.8 (t, J = 28.1 Hz), 138.6, 132.3, 124.3, 120.1, 114.7, 114.3, 111.0 (t, J = 234.9 Hz), 39.6. HRMS (ESI) m/z calcd for $C_{14}H_{12}F_2N_5OS$ $[M + H]^+$: 336.0725; found: 336.0729.

2-(3-(Difluoromethyl)-1-methyl-1H-pyrazol-4-yl*)-N-(pyridin*-4-yl*)thiazole-4-carboxamide* (**11 at**). White solid; yield: 68%; purity: 100%; m.p.: 183–185 °C; ^{1}H NMR (400 MHz, $CDCl_3$) δ 9.36 (s, 1H), 8.56 (dd, J = 4.9, 1.4 Hz, 2H), 8.18 (s, 1H), 7.97 (s, 1H), 7.64 (dd, J = 4.8, 1.5 Hz, 2H), 6.99 (t, J = 53.8 Hz, 1H), 4.01 (s, 3H). ^{13}C NMR (101 MHz, $CDCl_3$) δ 159.1, 158.5, 150.8, 149.3, 144.6, 142.9 (t, J = 27.9 Hz), 131.8, 124.3, 114.6, 113.6, 110.9 (t, J = 235.2 Hz), 39.7. HRMS (ESI) m/z calcd for $C_{14}H_{12}F_2N_5OS$ $[M + H]^+$: 336.0725; found: 336.0728.

N-(3-bromopyridin-4-yl*)-2-(3-(difluoromethyl)-1-methyl-1H-pyrazol*-4-yl*) thiazole-4-carboxamide* (**11au**). White solid; yield: 69%; purity: 99%; m.p.: 205–207 °C; ^{1}H NMR (400 MHz, $CDCl_3$) δ 10.05 (s, 1H), 8.71 (s, 1H), 8.57 (d, J = 5.5 Hz, 1H), 8.49 (d, J = 5.5 Hz, 1H), 8.21 (s, 1H), 7.95 (s, 1H), 7.18 (t, J = 53.8 Hz, 1H), 4.03 (s, 3H). ^{13}C NMR (101 MHz, $CDCl_3$) δ 159.0, 158.9, 151.9, 149.8, 149.3, 143.0 (t, J = 26.7 Hz), 142.5, 131.6, 124.5, 114.7, 114.5, 110.8, 110.4 (t, J = 235.8 Hz), 39.8. HRMS (ESI) m/z calcd for $C_{14}H_{11}BrF_2N_5OS$ $[M + H]^+$: 413.9830; found: 413.9830.

2-(3-(Difluoromethyl)-1-methyl-1H-pyrazol-4-yl*)-N-(pyrimidin*-4-yl*)thiazole-4-carboxamide* (**11av**). Light yellow solid; yield: 75%; purity: 100%; m.p.: 208–210 °C; ^{1}H NMR (400 MHz, $CDCl_3$) δ 9.78 (s, 1H), 8.95 (s, 1H), 8.70 (d, J = 5.7 Hz, 1H), 8.34 (d, J = 5.6 Hz, 1H), 8.25 (s, 1H), 8.07 (s, 1H), 6.98 (t, J = 53.8 Hz, 1H), 4.02 (s, 3H). ^{13}C NMR (101 MHz, $CDCl_3$) δ 159.5, 158.9, 158.6, 158.5, 156.8, 148.7, 142.9 (t, J = 28.2 Hz), 132.2, 125.3, 114.5, 111.0 (t, J = 234.9 Hz), 110.3, 39.7. HRMS (ESI) m/z calcd for $C_{13}H_{11}F_2N_6OS$ $[M + H]^+$: 337.0678; found: 337.0681.

2-(3-(Difluoromethyl)-1-methyl-1H-pyrazol-4-yl*)-N-(pyrazin*-2-yl*)thiazole-4-carboxamide* (**11aw**). Yellow solid; yield: 32%; purity: 99%; m.p.: 241–243 °C; ^{1}H NMR (400 MHz, $CDCl_3$) δ 9.73 (d, J = 1.2 Hz, 1H), 9.70 (s, 1H), 8.40 (d, J = 2.5 Hz, 1H), 8.37–8.33 (m, 1H), 8.25 (s, 1H), 8.04 (s, 1H), 7.00 (t, J = 53.8 Hz, 1H), 4.02 (s, 3H). ^{13}C NMR (101 MHz, $CDCl_3$) δ 158.7, 148.9, 148.0, 142.9 (d, J = 27.9 Hz), 142.4, 140.3, 136.9, 132.0, 124.9, 114.6, 110.9 (t, J = 235.0 Hz), 100.0, 39.7. HRMS (ESI) m/z calcd for $C_{13}H_{11}F_2N_6OS$ $[M + H]^+$: 337.0678; found: 337.0681.

2-(3-(Difluoromethyl)-1-methyl-1H-pyrazol-4-yl*)-N-(thiazol*-2-yl*)thiazole-4-carboxamide* (**11ax**). Yellow solid; yield: 78%; purity: 99%; m.p.: 214–216 °C; ^{1}H NMR (400 MHz, $CDCl_3$) δ 10.50 (s, 1H), 8.26 (s, 1H), 8.03 (s, 1H), 7.53 (d, J = 3.5 Hz, 1H), 7.06 (d, J = 3.5 Hz, 1H), 6.97 (t, J = 53.8 Hz, 1H), 4.02 (s, 3H). ^{13}C NMR (101 MHz, $CDCl_3$) δ 159.0, 158.0, 157.5, 147.80, 142.9 (t, J = 28.3 Hz), 138.0, 132.2, 125.1, 114.6, 114.1, 110.9 (t, J = 234.8 Hz), 39.7. HRMS (ESI) m/z calcd for $C_{12}H_{10}F_2N_5OS_2$ $[M + H]^+$: 342.0289; found: 342.0290.

2-(3-(Difluoromethyl)-1-methyl-1H-pyrazol-4-yl*)-N-(4-methylthiazol*-2-yl*) thiazole-4-carboxamide* (**11ay**). Light yellow solid; yield: 84%; purity: 98%; m.p.: 128–130 °C; ^{1}H NMR (400 MHz, $CDCl_3$) δ 10.43 (s, 1H), 8.24 (s, 1H), 8.00 (s, 1H), 6.96 (t, J = 53.8 Hz, 1H), 6.60 (d, J = 1.0 Hz, 1H), 4.01 (s, 3H), 2.39 (d, J = 0.9 Hz, 3H). ^{13}C NMR (101 MHz, $CDCl_3$) δ 157.9, 156.9, 155.7, 146.9, 146.7, 141.8 (t, J = 28.4 Hz), 131.1, 124.0, 113.6, 109.9 (t, J = 234.8 Hz), 107.6, 38.6, 16.1. HRMS (ESI) m/z calcd for $C_{13}H_{12}F_2N_5OS_2$ $[M + H]^+$: 356.0446; found: 356.0448.

N-(3-bromophenyl)-2-(3-(difluoromethyl)-1-methyl-1H-pyrazol-4-yl*)oxazole-4-carboxamide* (**11ba**). White solid; yield: 71%; purity: 100%; m.p.: 151–153 °C, ^{1}H NMR (400 MHz, $CDCl_3$) δ 8.65 (s, 1H), 8.25 (s, 1H), 7.99 (s, 1H), 7.93 (s, 1H), 7.59 (d, J = 7.8 Hz, 1H), 7.28 (d, J = 1.4 Hz, 1H), 7.22 (t, J = 7.9 Hz, 1H), 7.13 (t, J = 55.3 Hz, 1H), 4.01 (s, 3H). ^{13}C NMR (101 MHz, $CDCl_3$) δ 158.2, 155.6, 155.3, 143.7 (t, J = 26.4 Hz), 141.0, 138.6, 136.8, 132.2, 130.4, 127.6, 122.7, 118.3, 109.7 (t, J = 236.8 Hz), 108.5 (t, J = 2.5 Hz), 39.8. HRMS (ESI) m/z calcd for $C_{15}H_{12}BrF_2N_4O_2$ $[M + H]^+$: 397.0106; found: 397.0113.

2-(3-(Difluoromethyl)-1-methyl-1H-pyrazol-4-yl*)-N-(m-tolyl) oxazole-4-carboxamide* (**11bb**). Yellow solid; yield: 93%; purity: 99%; m.p.: 146–148 °C; ^{1}H NMR (400 MHz, $CDCl_3$) δ 8.64 (s, 1H), 8.23 (s, 1H), 7.97 (s, 1H), 7.48 (d, J = 6.6 Hz, 2H), 7.24 (t, J = 8.2 Hz, 1H), 7.15 (t, J = 53.7 Hz, 1H), 6.96 (d, J = 7.4 Hz, 1H), 3.97 (s, 3H), 2.36 (s, 3H). ^{13}C NMR (101 MHz, $CDCl_3$) δ 158.1, 155.2, 143.6 (t, J = 26.1 Hz), 140.8, 139.0, 137.2, 132.1, 128.9, 125.5, 120.5, 117.0, 109.7 (t, J = 236.3 Hz), 108.6 (t, J = 2.4 Hz), 39.7, 21.5. HRMS (ESI) m/z calcd for $C_{16}H_{15}F_2N_4O_2$ $[M + H]^+$: 333.1158; found: 333.1157.

2-(3-(Difluoromethyl)-1-methyl-1H-pyrazol-4-yl*)-N-(2-(trifluoromethyl)phenyl) oxazole-4-carboxamide* (**11bc**). White solid; yield: 58%; purity: 100%; m.p.: 157–159 °C; ^{1}H NMR (400 MHz, $CDCl_3$) δ 9.38 (s, 1H), 8.52 (d, J = 8.3 Hz, 1H), 8.27 (s, 1H), 7.99 (s, 1H), 7.66 (d, J = 7.9 Hz, 1H), 7.60 (t, J = 7.8 Hz, 1H), 7.28–7.22 (m, 1H), 7.17

(t, J = 53.8 Hz, 1H), 4.02 (s, 3H). ^{13}C NMR (101 MHz, $CDCl_3$) δ 158.3, 155.3, 143.9 (t, J = 25.9 Hz), 140.8, 136.8, 135.0, 133.0, 132.0, 126.2 (q, J = 5.3 Hz), 124.1 (q, J = 273.1 Hz), 124.3, 122.8, 119.5 (q, J = 29.9 Hz), 109.6 (t, J = 236.7 Hz), 108.5 (t, J = 2.7 Hz), 39.8. HRMS (ESI) m/z calcd for $C_{16}H_{12}F_5N_4O_2$ $[M + H]^+$: 387.0875; found: 387.0879.

*N-(3-bromophenyl)-5-(3-(difluoromethyl)-1-methyl-1H-pyrazol-*4-yl*)thiophene-2-carboxamide* (**11ca**). Yellow solid; yield: 98%; purity: 99%; m.p.: 103–105 °C; ^{1}H NMR (400 MHz, $CDCl_3$) δ 8.26 (s, 1H), 7.86 (s, 1H), 7.59–7.54 (m, 2H), 7.50 (d, J = 8.1 Hz, 1H), 7.22 (d, J = 7.9 Hz, 1H), 7.15 (dd, J = 9.5, 6.5 Hz, 2H), 6.74 (t, J = 53.9 Hz, 1H), 3.91 (s, 3H). ^{13}C NMR (101 MHz, $CDCl_3$) δ 160.2, 142.1 (t, J = 28.5 Hz), 138.9, 138.5, 137.1, 130.9, 130.3, 129.5, 127.6, 126.4 (t, J = 2.8 Hz), 123.4, 122.6, 119.0, 114.2, 111.6 (t, J = 234.1 Hz), 39.4. HRMS (ESI) m/z calcd for $C_{16}H_{13}BrF_2N_3OS$ $[M + H]^+$: 411.9925; found: 411.9924.

*5-(3-(Difluoromethyl)-1-methyl-1H-pyrazol-*4-yl*)-N-(m-tolyl) thiophene-2-carboxamide* (**11 cb**). Yellow solid; yield: 96%; purity: 99%; m.p.: 115–117 °C. ^{1}H NMR (400 MHz, $CDCl_3$) δ 8.08 (s, 1H), 7.55 (d, J = 2.2 Hz, 2H), 7.45 (s, 1H), 7.40 (d, J = 8.1 Hz, 1H), 7.19 (t, J = 7.8 Hz, 1H), 7.14 (d, J = 3.8 Hz, 1H), 6.93 (d, J = 7.5 Hz, 1H), 6.74 (t, J = 53.9 Hz, 1H), 3.89 (s, 3H), 2.29 (s, 3H). ^{13}C NMR (101 MHz, $CDCl_3$) δ 160.1, 142.1 (t, J = 28.3 Hz), 139.0, 137.8, 137.8, 137.6, 130.8, 129.1, 128.9, 126.3 (t, J = 2.7 Hz), 125.4, 121.1, 117.6, 114.3, 111.5 (t, J = 234.0 Hz), 39.4, 21.4. HRMS (ESI) m/z calcd for $C_{17}H_{16}F_2N_3OS$ $[M + H]^+$: 348.0977; found: 348.0978.

*N-(3-bromophenyl)-4-(3-(difluoromethyl)-1-methyl-1H-pyrazol-*4-yl*)benzamide* (**11da**). Yellow solid; yield: 91%; purity: 100%; m.p.: 110–112 °C. ^{1}H NMR (400 MHz, $CDCl_3$) δ 8.35 (s, 1H), 7.91 (s, 1H), 7.79 (d, J = 7.1 Hz, 2H), 7.58–7.44 (m, 4H), 7.24 (d, J = 7.6 Hz, 1H), 7.16 (t, J = 7.3 Hz, 1H), 6.73 (t, J = 54.1 Hz, 1H), 3.92 (s, 3H). ^{13}C NMR (101 MHz, $CDCl_3$) δ 165.8, 142.4 (t, J = 28.0 Hz), 139.3, 135.0, 132.9, 130.7, 130.3, 128.3, 127.6, 127.5, 123.3, 122.6, 120.9, 118.9, 111.9 (t, J = 233.9 Hz), 39.4. HRMS (ESI) m/z calcd for $C_{18}H_{15}BrF_2N_3O$ $[M + H]^+$: 406.0361; found: 406.0351.

*4-(3-(Difluoromethyl)-1-methyl-1H-pyrazol-*4-yl*)-N-(m-tolyl) benzamide* (**11 db**). White solid; yield: 95%; purity: 100%; m.p.: 133–135 °C, ^{1}H NMR (400 MHz, $CDCl_3$) δ 8.25 (s, 1H), 7.80 (d, J = 8.2 Hz, 2H), 7.49 (s, 2H), 7.47 (d, J = 8.3 Hz, 2H), 7.43 (d, J = 8.1 Hz, 1H), 7.19 (t, J = 7.8 Hz, 1H), 6.93 (d, J = 7.4 Hz, 1H), 6.72 (t, J = 54.1 Hz, 1H), 3.89 (s, 3H), 2.29 (s, 3H). ^{13}C NMR (101 MHz, $CDCl_3$) δ 165.6, 142.4 (t, J = 27.9 Hz), 139.0, 138.0, 134.6, 133.6, 130.7, 128.8, 128.2, 127.5, 125.4, 121.1, 121.1, 117.5, 111.8 (t, J = 233.9 Hz), 39.3, 21.5. HRMS (ESI) m/z calcd for $C_{19}H_{18}F_2N_3O$ $[M + H]^+$: 342.1412; found: 342.1418.

*4-(3-(Difluoromethyl)-1-methyl-1H-pyrazol-*4-yl*)-N-(2-(trifluoromethyl)phenyl)benzamide* (**11dc**). Light yellow solid; yield: 49%; purity: 100%; m.p.: 153–155 °C; ^{1}H NMR (400 MHz, $CDCl_3$) δ 8.41 (d, J = 8.2 Hz, 1H), 8.27 (s, 1H), 7.90 (dd, J = 8.4, 2.3 Hz, 2H), 7.68–7.59 (m, 5H), 7.27 (t, J = 7.4 Hz, 1H), 6.77 (t, J = 54.1 Hz, 1H), 3.97 (s, 3H). ^{13}C NMR (101 MHz, $CDCl_3$) δ 165.1, 142.6 (t, J = 28.1 Hz), 135.5, 135.4, 133.0, 132.8, 130.7, 128.6, 127.5, 126.2 (q, J = 5.3 Hz), 124.6, 124.3, 124.3 (q, J = 273.0 Hz), 120.9, 120.2 (q, J = 29.6 Hz), 111.8 (t, J = 234.0 Hz), 39.4. HRMS (ESI) m/z calcd for $C_{19}H_{15}F_5N_3O$ $[M + H]^+$: 396.1130; found: 396.1136.

*N-benzyl-4-(3-(difluoromethyl)-1-methyl-1H-pyrazol-*4-yl*)benzamide* (**11dd**). White solid; yield: 94%; purity: 100%; m.p.: 142–144 °C; ^{1}H NMR (400 MHz, $CDCl_3$) δ 7.80 (d, J = 8.1 Hz, 2H), 7.53 (d, J = 7.2 Hz, 2H), 7.50 (s, 1H), 7.34 (d, J = 4.2 Hz, 4H), 7.31–7.25 (m, 1H), 6.72 (t, J = 54.1 Hz, 1H), 6.64 (s, 1H), 4.63 (d, J = 5.6 Hz, 2H), 3.94 (s, 3H). ^{13}C NMR (101 MHz, $CDCl_3$) δ 167.0, 142.5 (t, J = 27.8 Hz), 138.2, 134.5, 133.0, 130.6, 128.8, 128.3, 127.9, 127.6, 127.4, 121.2, 111.8 (t, J = 234.0 Hz), 44.1, 39.4. HRMS (ESI) m/z calcd for $C_{19}H_{18}F_2N_3O$ $[M + H]^+$: 342.1412; found: 342.1415.

*4-(3-(Difluoromethyl)-1-methyl-1H-pyrazol-*4-yl*)-N-(3-(trifluoromethyl)phenyl) benzamide* (**11de**). White solid; yield: 23%; purity: 98%; m.p.: 136–138 °C; ^{1}H NMR (400 MHz, $CDCl_3$) δ 8.27 (s, 1H), 7.97 (s, 1H), 7.85 (d, J = 8.0 Hz, 3H), 7.55 (d, J = 8.3 Hz, 3H), 7.45 (t, J = 7.8 Hz, 1H), 7.39 (d, J = 7.5 Hz, 1H), 6.74 (t, J = 54.1 Hz, 1H), 3.95 (s, 3H). ^{13}C NMR (101 MHz, $CDCl_3$) δ 165.4, 142.6 (t, J = 28.2 Hz), 138.5, 135.3, 132.9, 131.6 (q, J = 32.4 Hz), 130.6, 129.7, 128.6, 127.5, 123.9 (q, J = 272.4 Hz), 123.2, 121.1 (q, J = 3.7 Hz), 121.0, 116.9 (q, J = 4.0 Hz), 111.9 (t, J = 234.0 Hz), 39.4. HRMS (ESI) m/z calcd for $C_{19}H_{15}F_5N_3O$ $[M + H]^+$: 396.1130; found: 396.1144.

*N-(3-bromophenyl)-3-(3-(difluoromethyl)-1-methyl-1H-pyrazol-*4-yl*)benzamide* (**11ea**). Yellow solid; yield: 56%; purity: 99%; m.p.: 150–152 °C; ^{1}H NMR (400 MHz, $CDCl_3$) δ 7.98 (s, 1H), 7.93 (s, 2H), 7.75 (d, J = 7.8 Hz, 1H), 7.69 (d, J = 7.8 Hz, 1H), 7.55 (d, J = 7.5 Hz, 2H), 7.49 (t, J = 7.7 Hz, 1H), 7.28 (d, J = 8.1 Hz, 1H), 7.22 (t, J = 8.0 Hz, 1H), 6.76 (t, J = 54.1 Hz, 1H), 3.95 (s, 3H). ^{13}C NMR (101 MHz, $CDCl_3$) δ 165.6, 142.4 (d, J = 28.0 Hz), 139.2, 134.9, 132.0, 131.8, 130.6, 130.4, 129.2, 127.6, 126.8, 125.7, 123.1, 122.7, 121.0, 118.6, 112.0 (t, J = 233.7 Hz), 39.4. HRMS (ESI) m/z calcd for $C_{18}H_{15}BrF_2N_3O$ $[M + H]^+$: 406.0361; found: 406.0361.

*3-(3-(Difluoromethyl)-1-methyl-1H-pyrazol-*4-yl*)-N-(m-tolyl) benzamide, white solid* (**11eb**). White solid; yield: 50%; purity: 100%; m.p.: 161–163 °C; ^{1}H NMR (400 MHz, $CDCl_3$) δ 7.94 (s, 2H), 7.76 (d, J = 7.8 Hz, 1H), 7.67 (d, J = 7.8 Hz, 1H), 7.55 (s, 1H), 7.53–7.41 (m, 3H), 7.25 (t, J = 7.8 Hz, 1H), 6.97 (d, J = 7.5 Hz, 1H), 6.76 (t, J = 54.1 Hz, 1H), 3.94 (s, 3H), 2.36 (s, 3H). ^{13}C NMR (101 MHz, $CDCl_3$) δ 165.5, 142.4 (t, J = 28.1 Hz), 139.1, 137.8, 135.5, 131.9, 131.5, 130.6, 129.1, 128.9, 126.8, 125.7, 125.4, 121.2, 120.8, 117.3, 111.9 (t, J = 233.8 Hz), 39.3, 21.5. HRMS (ESI) m/z calcd for $C_{19}H_{18}F_2N_3O$ $[M + H]^+$: 342.1412; found: 342.1417.

*3-(3-(Difluoromethyl)-1-methyl-1H-pyrazol-*4-yl*)-N-(2-(trifluoromethyl)phenyl) benzamide* (**11ec**). White solid; yield: 32%; purity: 100%; m.p.: 126–128 °C; ^{1}H NMR (400 MHz, $CDCl_3$) δ 8.43 (d, J = 8.2 Hz, 1H), 8.28 (s, 1H), 8.00 (s, 1H), 7.81 (d, J = 7.7 Hz, 1H), 7.72 (d, J = 7.7 Hz, 1H), 7.68–7.63 (m, 1H), 7.61 (d, J = 7.4 Hz, 2H), 7.55 (t, J = 7.8 Hz, 1H), 7.29 (d, J = 7.6 Hz, 1H), 6.77 (t, J = 54.1 Hz, 1H), 3.98 (s, 3H). ^{13}C NMR (101 MHz, $CDCl_3$) δ 165.3, 142.5 (t, J = 28.2 Hz), 135.4, 134.7, 133.0, 132.2, 132.0, 130.6, 129.4, 126.8, 126.2 (q, J = 5.3 Hz), 125.7, 124.6, 124.3, 124.2 (q, J = 272.9 Hz), 121.0, 120.2 (q, J = 29.6 Hz), 111.9 (t, J = 233.8 Hz), 39.4. HRMS (ESI) m/z calcd for $C_{19}H_{15}F_5N_3O$ $[M + H]^+$: 396.1130; found: 396.1134.

*N-benzyl-3-(3-(difluoromethyl)-1-methyl-1H-pyrazol-*4-yl*)benzamide* (**11ed**). Yellow solid; yield: 90%; purity: 100%; m.p.: 100–102 °C; ^{1}H NMR (400 MHz, $CDCl_3$) δ 7.88 (s, 1H), 7.69 (d, J = 7.8 Hz, 1H), 7.62 (d, J = 7.7 Hz, 1H), 7.47 (s, 1H), 7.39 (t, J = 7.7 Hz, 1H), 7.31 (d, J = 4.3 Hz, 4H), 7.26 (dt, J = 6.1, 3.8 Hz, 1H), 6.90 (t, J = 4.9 Hz, 1H), 6.70 (t, J = 54.1 Hz, 1H), 4.58 (d, J = 5.7 Hz, 2H), 3.86 (s, 3H). ^{13}C NMR (101 MHz, $CDCl_3$) δ 167.3, 142.3 (t, J = 27.8 Hz), 138.2, 134.8, 131.7, 131.3, 130.6, 128.9, 128.7, 127.8, 127.5, 126.9, 125.7, 121.2, 111.8 (t, J = 233.9 Hz), 44.0, 39.2. HRMS (ESI) m/z calcd for $C_{19}H_{18}F_2N_3O$ $[M + H]^+$: 342.1412; found: 342.1409.

*N-(3-bromophenyl)-3-(1-methyl-3-(trifluoromethyl)-1H-pyrazol-*4-yl*)benzamide* (**11ee**). White solid; yield: 58%; purity: 100%; m.p.: 177–179 °C; ^{1}H NMR (400 MHz, $CDCl_3$) δ 7.97 (s, 1H), 7.93 (t, J = 1.9 Hz, 1H), 7.85 (t, J = 1.6 Hz, 1H), 7.80–7.76 (m, 1H), 7.60 (d, J = 7.8 Hz, 1H), 7.57–7.53 (m, 2H), 7.51 (t, J = 7.7 Hz, 1H), 7.31–7.27 (m, 1H), 7.23 (t, J = 8.0 Hz, 1H), 3.98 (s, 3H). ^{13}C NMR (101 MHz, $CDCl_3$) δ 165.4, 139.1, 138.6 (q, J = 36.6 Hz), 134.9, 132.2, 132.2, 131.4, 131.1, 130.4, 129.2, 127.7, 127.3, 126.0, 123.1, 122.8, 121.5 (q, J = 269.4 Hz), 121.3, 118.6, 39.7. HRMS (ESI) m/z calcd for $C_{18}H_{14}BrF_3N_3O$ $[M + H]^+$: 424.0267; found: 424.0264.

*3-(1-Methyl-3-(trifluoromethyl)-1H-pyrazol-*4-yl*)-N-(m-tolyl) benzamide* (**11ef**). Light yellow solid; yield: 83%; purity: 100%; m.p.: 171–173 °C; ^{1}H NMR (400 MHz, $CDCl_3$) δ 8.01 (s, 1H), 7.86 (s, 1H), 7.78 (d, J = 7.3 Hz, 1H), 7.57 (d, J = 7.3 Hz, 1H), 7.53–7.41 (m, 4H), 7.23 (d, J = 7.5 Hz, 1H), 6.97 (d, J = 7.3 Hz, 1H), 3.95 (s, 3H), 2.35 (s, 3H). ^{13}C NMR (101 MHz, $CDCl_3$) δ 165.5, 139.1, 138.5 (q, J = 37.1 Hz), 137.8, 135.5, 131.8, 131.3, 131.2, 129.0, 128.9, 127.3, 126.0, 125.5, 121.5

(q, J = 269.5 Hz), 121.4, 120.9, 117.3, 39.6, 21.5. HRMS (ESI) m/z calcd for $C_{19}H_{17}F_3N_3O$ $[M + H]^+$: 360.1318; found: 360.1321.

*N-(2-isopropylphenyl)-3-(1-methyl-3-(trifluoromethyl)-1H-pyrazol-*4-yl*) benzamide* (**11eg**). White solid; yield: 79%; purity: 100%; m.p.: 142–144 °C; ^{1}H NMR (400 MHz, $CDCl_3$) δ 7.90 (s, 2H), 7.83 (d, J = 7.5 Hz, 1H), 7.78 (s, 1H), 7.61–7.54 (m, 2H), 7.50 (t, J = 7.7 Hz, 1H), 7.35–7.30 (m, 1H), 7.24–7.18 (m, 2H), 3.97 (s, 3H), 3.11 (dt, J = 13.6, 6.8 Hz, 1H), 1.28 (s, 3H), 1.26 (s, 3H). ^{13}C NMR (101 MHz, $CDCl_3$) δ 165.8, 140.8, 138.5 (q, J = 36.6 Hz), 135.4, 134.1, 131.8, 131.3, 131.2, 129.2, 127.2, 126.5, 126.3, 126.2, 125.8, 124.8, 121.6 (q, J = 269.4 Hz), 121.4, 39.7, 28.2, 23.0. HRMS (ESI) m/z calcd for $C_{21}H_{21}F_3N_3O$ $[M + H]^+$: 388.1631; found: 388.1632.

*3-(1,3-Dimethyl-1H-pyrazol-*4-yl*)-N-(m-tolyl)benzamide* (**11eh**). White solid; yield: 92%; purity: 100%; m.p.: 107–109 °C; ^{1}H NMR (400 MHz, $CDCl_3$) δ 8.46 (s, 1H), 7.83 (s, 1H), 7.67 (d, J = 7.5 Hz, 1H), 7.54 (s, 1H), 7.48 (d, J = 14.2 Hz, 1H), 7.46 (d, J = 14.6 Hz, 1H), 7.39 (t, J = 7.7 Hz, 1H), 7.36 (s, 1H), 7.21 (t, J = 7.8 Hz, 1H), 6.95 (d, J = 7.4 Hz, 1H), 3.75 (s, 3H), 2.36 (s, 3H), 2.32 (s, 3H). ^{13}C NMR (101 MHz, $CDCl_3$) δ 166.1, 145.6, 139.0, 138.1, 135.5, 134.2, 130.3, 129.2, 128.9, 126.3, 125.3, 124.4, 121.0, 120.1, 117.5, 38.6, 21.5, 13.2. HRMS (ESI) m/z calcd for $C_{19}H_{20}N_3O$ $[M + H]^+$: 306.1601; found: 306.1601.

4.2. Crystal structure determination

Single crystal X-ray diffraction data of compound **11ea** was collected on a Rigaku 007 Saturn 70 diffractionmeter using Mo Kα radiation (λ = 0.71073 Å). A total of 10241 reflections were collected in the range of $1.920° \le \theta \le 27.874°$ ($-10 \le h \le 10$, $-12 \le k \le 12$, $-15 \le l \le 15$) with 3976 unique reflections (R_{int} = 0.0674), of which 1694 had $I > 2\sigma(I)$ for refinements. The structure was directly solved by Olex2 1.2 program.

4.3. Evaluation of biological activity

4.3.1. In vitro antifungal assay

The antifungal activity of the title compounds **11aa-11eh** against *Alternaria solani*, *Botrytis cinerea*, *Cercospora arachidicola*, *Gibberella zeae*, *Phytophthora infestans* (Mont.) de Bary, *Physalospora piricola*, *Pellicularia sasakii*, *Rhizoctonia cerealis*, *Sclerotinia sclerotiorum* were evaluated *in vitro* at 50 μg/mL according to our reported method [21]. The commercial SDHI fungicide thifluzamide was used as a positive control. Compounds with good to excellent inhibitory activities were further assessed for their median effective concentration (EC_{50}) values according to our published procedures [21]. Three replicates were set up for each treatment.

4.3.2. In vivo antifungal assay

The *in vivo* antifungal activities of the target compounds against *Erysiphe graminis*, *Puccinia sorghi* Schw., *Pyricularia oryzae* Cav. and *Rhizoctonia solani* were assessed according to a previously reported method [28]. Thifluzamide was selected as a positive control.

4.3.3. SDH enzyme activity analysis

SDH catalyzed the dehydrogenation of succinic acid to fumaric acid. The removed hydrogen was transferred and reduced by phenazine dimethyl sulfuric acid (PMS) to reduce 2,6-dichlorophenol indophenol (DCPIP). The reduction rate of 2,6-DCPIP was determined by the change of absorbance at 600 nm, which represented the enzyme activity of SDH. The enzyme activity was calculated as per nmol 2,6-DCPIP consumed/min/mg protein as one unit (U/mg prot).

R. cerealis cultures were grown in Potato Dextrose Broth (PDB) medium on a reciprocal shaker (25 °C) for 5 days. One gram of the mycelium was obtained from PDB medium and ground in liquid nitrogen. The resultant powder was resuspended in mitochondrial extraction buffer (5 mL of reagent 1 and 50 μL of reagent 2 (BC0955, solarbio, Beijing)). After shaking and mixing at 4 °C for 2 min, the supernatant was collected for protein interaction analysis by centrifugation (11000g, 4 °C for 10 min, 2 times). The mitochondrial suspensions were diluted in Phosphate Buffered Saline (PBS) buffer. And the tested compounds concentrations ranged between 0.05 and 20 mg/L (six concentrations + DMSO control). The SDH enzymatic activity was measured according to our previously reported method [5]. The IC_{50} values of representative compounds were calculated by GraphPad Prim version 6.02 program.

4.4. Fluorescence quenching analysis of SDH

The discovery and identification of new targets is an effective basis for the development of novel pesticides [29]. Target validation is also an important mean to expand the diversity of lead compounds [30]. The mitochondria of *R. cerealis* were extracted according to the operation instruction (BC0955, solarbio, Beijing). The mitochondrial suspensions were diluted in PBS buffer (pH = 7.4, 136.89 m mol/L NaCl, 2.67 m mol/L KCl, 8.1 m mol/L Na_2HPO_4, and 1.76 m mol/L KH_2PO_4), and then add 1 mL of the diluted mitochondrial suspension to the quartz cuvette. Fluorescence emission spectra were recorded at a wavelength of 300–420 nm with an excitation wavelength of 280 nm at 4 °C, and the emission band width was set at 10 nm with medium sensitivity. The solution of compound **11ea** and controls were added into the suspension for fluorescence determination respectively, 1 μL each time for 5 times, each intermission for 1 min. The concentrations of **11ea** and controls were within a range of 0–5 μg/mL, with uniform 2 × dilution factor steps (0 μg/mL + four concentrations). Thifluzamide and tricyclazole were used as a positive and a negative control, respectively.

4.5. Homology modeling and molecular docking

The crystal structure of *R. cerealis* SDH has not been reported yet; therefore, a SDH structure of *R. cerealis* was constructed by homology modeling. The target protein sequences of SDHB, SDHC and SDHD (entry code: A0A173DSZ5, A0A173DSZ3 and A0A173DT05, respectively) were obtained from uniprot website (https://www.uniprot.org/). Then, the template proteins (entry code: 4YXD and 1YQ3) were selected from the PDB (Protein Data Bank) through BLASTp. Homology modeling was performed on Modeller 9.18 [31,32]. Since the binding site of SDH was just constructed by SDHB, SDHC and SDHD, SDHA of *R. cerealis* SDH was not constructed in this model. The individual sub-models (SDHB, SDHC and SDH) were then assembled by superimposing on the template (4YXD) using Chimera 1.13.1 [33].

The docking binding center of predicted *Rc*SDH was defined by Autodock Tools-1.5.6 according to the co-crystallized ligand flutolanil (4YXD) [34,35]. The docking pocket was centered on the ligand, which grid size was set 20 × 20 × 20 and the grid space was 0.375 Å. The crystal structure of **11ea** was applied in this experiment. Thifluzamide and other selected compounds were optimized according to the ligand minimization protocol. During the process, the ligands were allowed to be flexible while the receptor was held rigid [36]. The molecular docking analysis was operated on PyMOL.

Declaration of competing interest

The authors declare that they have no known competing financial interests or personal relationships that could have appeared to influence the work reported in this paper.

Acknowledgments

This work was supported in part by the National Natural Science Foundation of China (No. 31872007), the Fundamental Research Funds for the Central Universities, Nankai University (No. 63191743), the Tianjin Natural Science Foundation (No. 18JCZDJC33500), the International Science & Technology Cooperation Program of China (No. 2014DFR41030), the Tianjin Development Program for Innovation and Entrepreneurship.

Dedicated to the 100th Anniversary of Chemistry at Nankai University.

Appendix A. Supplementary data

Supplementary data to this article can be found online at https://doi.org/10.1016/j.ejmech.2021.113230.

References

[1] L. Chen, Y.J. Zhu, Z.J. Fan, X.F. Guo, Z.M. Zhang, J.H. Xu, Y.Q. Song, M.Y. Yurievich, N.P. Belskaya, V.A. Bakulev, Synthesis of 1,2,3-thiadiazole and thiazole-based strobilurins as potent fungicide candidates, J. Agric. Food Chem. 65 (2017) 745–751.

[2] H. Sierotzki, G. Scalliet, A review of current knowledge of resistance aspects for the next-generation succinate dehydrogenase inhibitor fungicides,, Phytopathology 103 (2013) 880–887.

[3] G. Scalliet, J. Bowler, T. Luksch, L. Kirchhofer-Allan, D. Steinhauer, K. Ward, M. Niklaus, A. Verras, M. Csukai, A. Daina, Mutagenesis and functional studies with succinate dehydrogenase inhibitors in the wheat pathogen *Mycosphaerella graminicola*, PloS One 7 (2012) e35429.

[4] C.E. Keohane, A.D. Steele, C. Fetzer, J. Khowsathit, D. Van Tyne, L. Moynié, M.S. Gilmore, J. Karanicolas, S.A. Sieber, W.M. Wuest, Promysalin elicits species-selective inhibition of by targeting succinate dehydrogenase, J. Am. Chem. Soc. 140 (2018) 1774–1782.

[5] X.F. Guo, B. Zhao, Z.J. Fan, D.Y. Yang, N.N. Zhang, Q.F. Wu, B. Yu, S. Zhou, T.A. Kalinina, N.P. Belskaya, Discovery of novel thiazole carboxamides as antifungal succinate dehydrogenase inhibitors, J. Agric. Food Chem. 67 (2019) 1647–1655.

[6] Z.Z. Yan, A.P. Liu, M.Z. Huang, M.H. Liu, H. Pei, L. Huang, H.B. Yi, W.D. Liu, A.X. Hu, Design, synthesis, DFT study and antifungal activity of the derivatives of pyrazole carboxamide containing thiazole or oxazole ring, Eur. J. Med. Chem. 149 (2018) 170–181.

[7] Z.J. Wang, Y. Gao, Y.L. Hou, C. Zhang, S.J. Yu, Q. Bian, Z.M. Li, W.G. Zhao, Design, synthesis, and fungicidal evaluation of a series of novel 5-methyl-1*H*-1,2,3-trizole-4-carboxyl amide and ester analogues, Eur. J. Med. Chem. 86 (2014) 87–94.

[8] F. Wen, H. Jin, K. Tao, T.P. Hou, Design, synthesis and antifungal activity of novel furan carboxamide derivatives, Eur. J. Med. Chem. 120 (2016) 244–251.

[9] H. Wang, X. Gao, X. Zhang, H. Jin, K. Tao, T. Hou, Design, synthesis and antifungal activity of novel fenfuram-diarylamine hybrids, Bioorg. Med. Chem. Lett 27 (2017) 90–93.

[10] H. Wang, B. Huwaimel, K. Verma, J. Miller, T. Germain, N. Kinarivala, D. Pappas, P.S. Brookes, P.C. Trippier, Synthesis, Antineoplastic Evaluation, Of mitochondrial complex II (succinate dehydrogenase) inhibitors derived from Atpenin A5, ChemMedChem 12 (2017) 1033–1044.

[11] G. White, Substituted benzanilides: structural variation and inhibition of complex II activity in mitochondria from a wild-type strain and a carboxin-selected mutant strain of *Ustilago maydis*, Pestic. Biochem. Physiol. 27 (1987) 249–260.

[12] A. Amiri, S.M. Heath, N.A. Peres, Resistance to fluopyram, fluxapyroxad, and penthiopyrad in *Botrytis cinerea* from strawberry, Plant Dis. 98 (2014) 532–539.

[13] H. Ishii, T. Miyamoto, S. Ushio, M. Kakishima, Lack of cross-resistance to a novel succinate dehydrogenase inhibitor, fluopyram, in highly boscalid-resistant isolates of *Corynespora cassiicola* and *Podosphaera xanthii*, Pest Manag. Sci. 67 (2011) 474–482.

[14] B.M. Chougala, S. Samundeeswari, M. Holiyachi, L.A. Shastri, S. Dodamani, S. Jalalpure, S.R. Dixit, S.D. Joshi, V.A. Sunagar, Synthesis, characterization and molecular docking studies of substituted 4-coumarinylpyrano [2,3-*c*] pyrazole derivatives as potent antibacterial and anti-inflammatory agents, Eur. J. Med. Chem. 125 (2017) 101–116.

[15] A. Kamal, A.B. Shaik, N. Jain, C. Kishor, A. Nagabhushana, B. Supriya, G.B. Kumar, S.S. Chourasiya, Y. Suresh, R.K. Mishra, Design and synthesis of pyrazole–oxindole conjugates targeting tubulin polymerization as new anticancer agents, Eur. J. Med. Chem. 92 (2015) 501–513.

[16] Y.H. Ma, S. Liang, Y.C. Zhang, D.W. Yang, R.F. Wang, Development of antifungal pesticides from protein kinase inhibitor-based anticancer agents, Eur. J. Med. Chem. 148 (2018) 349–358.

[17] Ş, G. Küçükgüzel, S. Şenkardeş, Recent advances in bioactive pyrazoles, Eur. J. Med. Chem. 97 (2015) 786–815.

[18] M.F. Khan, M.M. Alam, G. Verma, W. Akhtar, M. Akhter, M. Shaquiquzzaman, The therapeutic voyage of pyrazole and its analogs: a review,, Eur. J. Med. Chem. 120 (2016) 170–201.

[19] B. Yu, L.X. Cao, Z.J. Fan, Z.S. Hao, D.Y. Yang, X.F. Guo, N.N. Zhang, S. Zhou, V.A. Bakulev, Design, synthesis, and evaluation of fungicidal activity of novel pyrazole-thiazole carboxamides as succinate dehydrogenase inhibitors, J. Agric. Food Chem. 68 (2020) 7093–7102.

[20] K. Ninomiya, T. Shioiri, S.-i. Yamada, Phosphorus in organic synthesis—VII: diphenyl phosphorazidate (DPPA). A new convenient reagent for a modified curtius reaction,, Tetrahedron 30 (1974) 2151–2157.

[21] Z.J. Fan, Z.K. Yang, H.K. Zhang, N. Mi, H. Wang, F. Cai, X. Zuo, Q.X. Zheng, H.B. Song, Synthesis, crystal structure, and biological activity of 4-methyl-1,2,3-thiadiazole-containing 1,2,4-triazolo[3,4-*b*][1,3,4]thiadiazoles, J. Agric. Food Chem. 58 (2009) 2630–2636.

[22] B. Zhao, S.J. Fan, Z.J. Fan, H.X. Wang, N.L. Zhang, X.F. Guo, D.Y. Yang, Q.F. Wu, B. Yu, S. Zhou, Discovery of pyruvate kinase as a novel target of new fungicide candidate 3-(4-methyl-1,2,3-thiadiazolyl)-6-trichloromethyl-[1,2,4]- triazolo-[3,4-*b*][1,3,4]-thiadizole, J. Agric. Food Chem. 66 (2018) 12439–12452.

[23] N.L. Zhang, B. Zhao, Z.J. Fan, D.Y. Yang, X.F. Guo, Q.F. Wu, B. Yu, S. Zhou, H.X. Wang, Systematic identification of genes associated with plant growth–defense tradeoffs under JA signaling in *Arabidopsis*, Planta 251 (2020) 43.

[24] H.Y. Sun, C.Q. Lu, W. Li, Y.Y. Deng, H.G. Chen, Homozygous and heterozygous point mutations in succinate dehydrogenase subunits b, c and d of *Rhizoctonia cerealis* conferring resistance to thifluzamide, Pest Manag. Sci. 73 (2017) 896–903.

[25] D. Mares, C. Romagnoli, E. Andreotti, M. Manfrini, C.B. Vicentini, Synthesis and antifungal action of new tricyclazole analogues, J. Agric. Food Chem. 52 (2004) 2003–2009.

[26] L. Geist, M. Mayer, X.-L. Cockcroft, B. Wolkerstorfer, D. Kessler, H. Engelhardt, D.B. McConnell, R. Konrat, Direct NMR probing of hydration shells of protein ligand interfaces and its application to drug design, J. Med. Chem. 60 (2017) 8708–8715.

[27] C.J. Goddard, Antiinflammatory 1-phenylpyrazole-4-heteroarylalkanoic acids, J. Heterocycl. Chem. 28 (1991) 1607–1612.

[28] Y.Q. Xie, Y.B. Huang, J.S. Liu, L.Y. Ye, L.M. Che, S. Tu, C.L. Liu, Design, synthesis and structure–activity relationship of novel oxime ether strobilurin derivatives containing substituted benzofurans, Pest Manag. Sci. 71 (2015) 404–414.

[29] B. Zhao, L. Chen, N.N. Zhang, Z.J. Fan, General summary of novel fungicide target identification and its targeted candidate design, Chin. J. Pesticide Sci. 20 (2018) 397–407.

[30] B. Zhao, H.X. Wang, Z.J. Fan, Q.F. Wu, X.F. Guo, N.N. Zhang, D.Y. Yang, B. Yu, S. Zhou, Mode of action for a new potential fungicide candidate, 3-(4-Methyl-1, 2, 3-thiadiazolyl)-6-trichloromethyl-[1, 2, 4]-triazolo-[3, 4-*b*][1, 3, 4]-thiadiazole by iTRAQ, Food and Agric, Immunol. 30 (2019) 533–547.

[31] M.A. Martí-Renom, A.C. Stuart, A. Fiser, R. Sánchez, F. Melo, A. Šali, Comparative protein structure modeling of genes and genomes, Annu. Rev. Biophys. Biomol. Struct. 29 (2000) 291–325.

[32] A. Šali, T.L. Blundell, Comparative protein modelling by satisfaction of spatial restraints, J. Mol. Biol. 234 (1993) 779–815.

[33] E.F. Pettersen, T.D. Goddard, C.C. Huang, G.S. Couch, D.M. Greenblatt, E.C. Meng, T.E. Ferrin, UCSF Chimera—a visualization system for exploratory research and analysis, J. Comput. Chem. 25 (2004) 1605–1612.

[34] E.D. Muzio, D. Toti, F. Polticelli, DockingApp: a user friendly interface for facilitated docking simulations with AutoDock Vina, J. Comput. Aided Mol. Des. 31 (2017) 213–218.

[35] G.M. Morris, D.S. Goodsell, R. Huey, A.J. Olson, Distributed automated docking of flexible ligands to proteins: parallel applications of AutoDock 2.4, J. Comput. Aided Mol. Des. 10 (1996) 293–304.

[36] O. Trott, A.J. Olson, AutoDock Vina: improving the speed and accuracy of docking with a new scoring function, efficient optimization, and multithreading, J. Comput. Chem. 31 (2010) 455–461.